

# Approximations in Bases

# 9

It is time to wonder why we are constructing so many different orthonormal bases. In signal processing, orthogonal bases are of interest because they can provide sparse representations of certain types of signals with few vectors. Compression and denoising are applications studied in Chapters 10 and 11.

Approximation theory studies the error produced by different approximation schemes. Classic sampling theorems are linear approximations that project the analog signal over low-frequency vectors chosen a priori in a basis. The discrete signal representation may be further reduced with a linear projection over the first few vectors of an orthonormal basis. However, better nonlinear approximations are obtained by choosing the approximation vectors depending on the signal. In a wavelet basis, these nonlinear approximations locally adjust the approximation resolution to the signal regularity.

Approximation errors depend on the signal regularity. For uniformly regular signals, linear and nonlinear approximations perform similarly, whether in a wavelet or in a Fourier basis. When the signal regularity is not uniform, nonlinear approximations in a wavelet basis can considerably reduce the error of linear approximations. This is the case for piecewise regular signals or bounded variation signals and images. Geometric approximations of piecewise regular images with regular edge curves are studied with adaptive triangulations and curvelets.

---

## 9.1 LINEAR APPROXIMATIONS

Analog signals are discretized in Section 3.1.3 with inner products in a basis. In the following sections we compute the resulting linear approximation error in wavelet and Fourier bases, which depends on the uniform signal regularity. For signals modeled as realizations of a random vector, in Section 9.1.4 we prove that the optimal basis is the Karhunen-Loëve basis (principal components), which diagonalizes the covariance matrix.

### 9.1.1 Sampling and Approximation Error

Approximation errors of linear sampling processes are related to the error of linear approximations in an orthogonal basis. These errors are computed from the decay of signal coefficients in this basis.

An analog signal  $f(t)$  is discretized with a low-pass filter  $\bar{\phi}_s(t)$  and a uniform sampling interval  $s$ :

$$f \star \bar{\phi}_s(ns) = \int_{-\infty}^{+\infty} f(u) \bar{\phi}_s(ns - u) du = \langle f(t), \phi_s(t - ns) \rangle, \quad (9.1)$$

with  $\bar{\phi}_s(t) = \phi_s(-t)$ . Let us consider an analog signal of compact support, normalized to  $[0, 1]$ . At a resolution  $N$  corresponding to  $s = N^{-1}$ , the discretization is performed over  $N$  functions  $\{\phi_n(t) = \phi_s(t - ns)\}_{0 \leq n < N}$  that are modified at the boundaries to maintain their support in  $[0, 1]$ . They define a Riesz basis of an approximation space  $\mathbf{U}_N \subset \mathbf{L}^2[0, 1]$ . The best linear approximation of  $f$  in  $\mathbf{U}_N$  is the orthogonal projection  $f_N$  of  $f$  in  $\mathbf{U}_N$ , recovered with the biorthogonal basis  $\{\tilde{\phi}_n(t)\}_{1 \leq n \leq N}$ :

$$f_N(t) = \sum_{n=0}^{N-1} \langle f, \phi_n \rangle \tilde{\phi}_n(t). \quad (9.2)$$

To compute the approximation error  $\|f - f_N\|$ , we introduce an orthonormal basis  $\mathcal{B} = \{g_m\}_{m \in \mathbb{N}}$  of  $\mathbf{L}^2[0, 1]$ , with  $N$  vectors  $\{g_m\}_{0 \leq m < N}$  defining an orthogonal basis of the same approximation space  $\mathbf{U}_N$ . Fourier and wavelet bases provide such bases for many classic approximation spaces. The orthogonal projection  $f_N$  of  $f$  in  $\mathbf{U}_N$  can be decomposed on the first  $N$  vectors of this basis:

$$f_N = \sum_{m=0}^{N-1} \langle f, g_m \rangle g_m.$$

Since  $\mathcal{B}$  is an orthonormal basis of  $\mathbf{L}^2[0, 1]$ ,  $f = \sum_{m=0}^{+\infty} \langle f, g_m \rangle g_m$ , so

$$f - f_N = \sum_{m=N}^{+\infty} \langle f, g_m \rangle g_m,$$

and the resulting approximation error is

$$\varepsilon_l(N, f) = \|f - f_N\|^2 = \sum_{m=N}^{+\infty} |\langle f, g_m \rangle|^2. \quad (9.3)$$

The fact that  $\|f\|^2 = \sum_{m=0}^{+\infty} |\langle f, g_m \rangle|^2 < +\infty$  implies that the error decays to zero:

$$\lim_{N \rightarrow +\infty} \varepsilon_l(N, f) = 0.$$

However, the decay rate of  $\varepsilon_l(N, f)$  as  $N$  increases depends on the decay of  $|\langle f, g_m \rangle|$  as  $m$  increases. Theorem 9.1 gives equivalent conditions on the decay of  $\varepsilon_l(N, f)$  and  $|\langle f, g_m \rangle|$ .

**Theorem 9.1.** For any  $s > 1/2$ , there exists  $A, B > 0$  such that if  $\sum_{m=0}^{+\infty} |m|^{2s} |\langle f, g_m \rangle|^2 < +\infty$ , then

$$A \sum_{m=0}^{+\infty} m^{2s} |\langle f, g_m \rangle|^2 \leq \sum_{N=0}^{+\infty} N^{2s-1} \varepsilon_l(N, f) \leq B \sum_{m=0}^{+\infty} m^{2s} |\langle f, g_m \rangle|^2, \quad (9.4)$$

and thus  $\varepsilon_l(N, f) = o(N^{-2s})$ .

**Proof.** By inserting (9.3), we compute

$$\sum_{N=0}^{+\infty} N^{2s-1} \varepsilon_l(N, f) = \sum_{N=0}^{+\infty} \sum_{m=N}^{+\infty} N^{2s-1} |\langle f, g_m \rangle|^2 = \sum_{m=0}^{+\infty} |\langle f, g_m \rangle|^2 \sum_{N=0}^m N^{2s-1}.$$

For any  $s > 1/2$ ,

$$\int_0^m x^{2s-1} dx \leq \sum_{N=0}^m N^{2s-1} \leq \int_1^{m+1} x^{2s-1} dx,$$

which implies that  $\sum_{N=0}^m N^{2s-1} \sim m^{2s}$  and thus proves (9.4).

To verify that  $\varepsilon_l(N, f) = o(N^{-2s})$ , observe that  $\varepsilon_l(m, f) \geq \varepsilon_l(N, f)$  for  $m \leq N$ , so

$$\varepsilon_l(N, f) \sum_{m=N/2}^{N-1} m^{2s-1} \leq \sum_{m=N/2}^{N-1} m^{2s-1} \varepsilon_l(m, f) \leq \sum_{m=N/2}^{+\infty} m^{2s-1} \varepsilon_l(m, f). \quad (9.5)$$

Since  $\sum_{m=1}^{+\infty} m^{2s-1} \varepsilon_l(m, f) < +\infty$ , it follows that

$$\lim_{N \rightarrow +\infty} \sum_{m=N/2}^{+\infty} m^{2s-1} \varepsilon_l(m, f) = 0.$$

Moreover, there exists  $C > 0$  such that  $\sum_{m=N/2}^{N-1} m^{2s-1} \geq C N^{2s}$ , so (9.5) implies that  $\lim_{N \rightarrow +\infty} \varepsilon_l(N, f) N^{2s} = 0$ . ■

This theorem proves that the linear approximation error of  $f$  in basis  $\mathcal{B}$  decays faster than  $N^{-2s}$  if  $f$  belongs to the space

$$\mathbf{W}_{\mathcal{B},s} = \left\{ f \in \mathbf{H} : \sum_{m=0}^{+\infty} m^{2s} |\langle f, g_m \rangle|^2 < +\infty \right\}.$$

One can also prove that this linear approximation is asymptotically optimal over this space [20]. Indeed, there exists nonlinear or nonlinear approximation scheme with error decays that are at least like  $N^{-\alpha}$ , with  $\alpha > 2s$ , for all  $f \in \mathbf{W}_{\mathcal{B},s}$ .

In the next sections we prove that if  $\mathcal{B}$  is a Fourier or wavelet basis, then  $\mathbf{W}_{\mathcal{B},s}$  is a Sobolev space, and therefore that linear approximations of Sobolev functions are optimal in Fourier and wavelet bases. However, we shall also see that for more complex functions, the linear approximation of  $f$  from the first  $N$  vectors of  $\mathcal{B}$  is not always precise because these vectors are not necessarily the best ones to approximate  $f$ . Nonlinear approximations calculated with vectors chosen adaptively depending on  $f$  are studied in Section 9.2.

### 9.1.2 Linear Fourier Approximations

The Shannon-Whittaker sampling theorem performs a perfect low-pass filter that keeps the signal low frequencies. Thus, it is equivalent to a linear approximation over the lower frequencies of a Fourier basis. Linear Fourier approximations are asymptotically optimal for uniformly regular signals. The approximation error is related to the Sobolev differentiability. It is also calculated for nonuniform regular signals, such as discontinuous signals having a bounded total variation.

Theorem 3.6 proves (modulo a change of variable) that  $\{e^{i2\pi mt}\}_{m \in \mathbb{Z}}$  is an orthonormal basis of  $L^2[0, 1]$ . Thus, we can decompose  $f \in L^2[0, 1]$  in the Fourier series

$$f(t) = \sum_{m=-\infty}^{+\infty} \langle f(u), e^{i2\pi mu} \rangle e^{i2\pi mt}, \quad (9.6)$$

with

$$\langle f(u), e^{i2\pi mu} \rangle = \int_0^1 f(u) e^{-i2\pi mu} du.$$

The decomposition (9.6) defines a periodic extension of  $f$  for all  $t \in \mathbb{R}$ . The decay of the Fourier coefficients  $|\langle f(u), e^{i2\pi mu} \rangle|$  as  $m$  increases depends on the regularity of this periodic extension.

The linear approximation of  $f \in L^2[0, 1]$  by the  $N$  sinusoids of lower frequencies is obtained by a linear filtering that sets all higher frequencies to zero:

$$f_N(t) = \sum_{|m| \leq N/2} \langle f(u), e^{i2\pi mu} \rangle e^{i2\pi mt}.$$

It projects  $f$  in space  $U_N$  of functions having Fourier coefficients that are zero above the frequency  $N\pi$ .

#### Error Decay versus Sobolev Differentiability

The decay of the linear Fourier approximation error depends on the Sobolev differentiability. The regularity of  $f$  can be measured by the number of times it is differentiable. Sobolev differentiability extends derivatives to nonintegers with a Fourier decay condition. To avoid boundary issues, we first consider functions  $f(t)$  defined for all  $t \in \mathbb{R}$ .

Recall that the Fourier transform of the derivative  $f'(t)$  is  $i\omega \hat{f}(\omega)$ . The Plancherel formula proves that  $f' \in L^2(\mathbb{R})$  if

$$\int_{-\infty}^{+\infty} |\omega|^2 |\hat{f}(\omega)|^2 d\omega = 2\pi \int_{-\infty}^{+\infty} |f'(t)|^2 dt < +\infty.$$

This suggests replacing the usual pointwise definition of the derivative by a definition based on the Fourier transform. We say that  $f \in L^2(\mathbb{R})$  is differentiable in the *sense of Sobolev* if

$$\int_{-\infty}^{+\infty} |\omega|^2 |\hat{f}(\omega)|^2 d\omega < +\infty. \quad (9.7)$$

This integral imposes that  $|\hat{f}(\omega)|$  has a sufficiently fast decay when the frequency  $\omega$  goes to  $+\infty$ . As in Section 2.3.1, the regularity of  $f$  is measured from the asymptotic decay of its Fourier transform.

This definition is generalized for any  $s > 0$ . Space  $\mathbf{W}^s(\mathbb{R})$  of  $s$  times differentiable Sobolev functions is the space of functions  $f \in \mathbf{L}^2(\mathbb{R})$  having a Fourier transform that satisfies [67]

$$\int_{-\infty}^{+\infty} |\omega|^{2s} |\hat{f}(\omega)|^2 d\omega < +\infty. \quad (9.8)$$

If  $s > n + 1/2$ , then one can verify (Exercise 9.7) that  $f$  is  $n$  times continuously differentiable.

Let  $\mathbf{W}^s[0, 1]$  be the space of functions in  $\mathbf{L}^2[0, 1]$  that can be extended outside  $[0, 1]$  into a function  $f \in \mathbf{W}^s(\mathbb{R})$ . To avoid border problems at  $t = 0$  or at  $t = 1$ , let us consider functions  $f$  that have supports that are strictly included in  $(0, 1)$ . A simple regular extension on  $\mathbb{R}$  is obtained by setting its value to 0 outside  $[0, 1]$ , and  $f \in \mathbf{W}^s[0, 1]$  if this extension is in  $\mathbf{W}^s(\mathbb{R})$ . In this case, one can prove (not trivial) that the Sobolev integral condition (9.8) reduces to a discrete sum, meaning that  $f \in \mathbf{W}^s[0, 1]$  if and only if

$$\sum_{m=-\infty}^{+\infty} |m|^{2s} |\langle f(u), e^{i2\pi mu} \rangle|^2 < +\infty. \quad (9.9)$$

For such differentiable functions in the sense of Sobolev, Theorem 9.2 computes the approximation error

$$\varepsilon_l(N, f) = \|f - f_N\|^2 = \int_0^1 |f(t) - f_N(t)|^2 dt = \sum_{|m|>N/2} |\langle f(u), e^{i2\pi mu} \rangle|^2. \quad (9.10)$$

**Theorem 9.2.** Let  $f \in \mathbf{L}^2[0, 1]$  be a function with support strictly included in  $(0, 1)$ . Then  $f \in \mathbf{W}^s[0, 1]$  if and only if

$$\sum_{N=1}^{+\infty} N^{2s} \frac{\varepsilon_l(N, f)}{N} < +\infty, \quad (9.11)$$

which implies  $\varepsilon_l(N, f) = o(N^{-2s})$ . ■

The proof relies on the fact that functions in  $\mathbf{W}^s[0, 1]$  with a support in  $(0, 1)$  are characterized by (9.9). Therefore, this theorem is a consequence of Theorem 9.1. Thus, the linear Fourier approximation decays quickly if and only if  $f$  has a large regularity exponent  $s$  in the sense of Sobolev.

### Discontinuities and Bounded Variation

If  $f$  is discontinuous, then  $f \notin \mathbf{W}^s[0, 1]$  for any  $s > 1/2$ . Thus, Theorem 9.2 proves that  $\varepsilon_l(N, f)$  can decay like  $N^{-\alpha}$  only if  $\alpha \leq 1$ . For bounded variation functions,

which are introduced in Section 2.3.3, Theorem 9.3 proves that  $\varepsilon_l(N, f) = O(N^{-1})$ . A function has a bounded variation if

$$\|f\|_V = \int_0^1 |f'(t)| dt < +\infty.$$

The derivative must be taken in the sense of distributions because  $f$  may be discontinuous. If  $f = \mathbf{1}_{[0,1/2]}$ , then  $\|f\|_V = 2$ . Recall that  $a[N] \sim b[N]$  if  $a[N] = O(b[N])$  and  $b[N] = O(a[N])$ .

**Theorem 9.3.**

- If  $\|f\|_V < +\infty$ , then  $\varepsilon_l(N, f) = O(\|f\|_V^2 N^{-1})$ .
- If  $f = C \mathbf{1}_{[0,1/2]}$ , then  $\varepsilon_l(N, f) \sim \|f\|_V^2 N^{-1}$ .

**Proof.** If  $\|f\|_V < +\infty$ , then

$$\begin{aligned} |\langle f(u), \exp(i2m\pi u) \rangle| &= \left| \int_0^1 f(u) \exp(-i2m\pi u) du \right| \\ &= \left| \int_0^1 f'(u) \frac{\exp(-i2m\pi u)}{-i2m\pi} dt \right| \leq \frac{\|f\|_V}{2|m|\pi}. \end{aligned}$$

Thus,

$$\varepsilon_l(N, f) = \sum_{|m|>N/2} |\langle f(u), \exp(i2m\pi u) \rangle|^2 \leq \frac{\|f\|_V^2}{4\pi^2} \sum_{|m|>N/2} \frac{1}{m^2} = O(\|f\|_V^2 N^{-1}).$$

If  $f = C \mathbf{1}_{[0,1/2]}$ , then  $\|f\|_V = 2C$  and

$$|\langle f(u), \exp(i2m\pi u) \rangle| = \begin{cases} 0 & \text{if } m \neq 0 \text{ is even} \\ C/(\pi|m|) & \text{if } m \text{ is odd,} \end{cases}$$

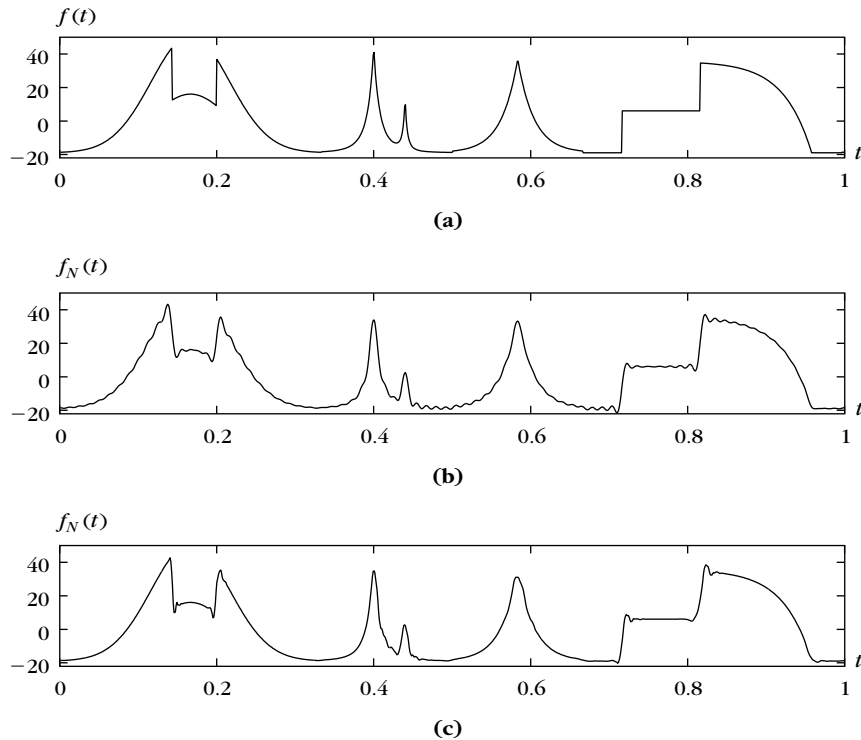
so  $\varepsilon_l(N, f) \sim C^2 N^{-1}$ . ■

This theorem shows that when  $f$  is discontinuous with bounded variations, then  $\varepsilon_l(N, f)$  decays typically like  $N^{-1}$ . Figure 9.1(b) shows a bounded variation signal approximated by Fourier coefficients of lower frequencies. The approximation error is concentrated in the neighborhood of discontinuities where the removal of high frequencies creates Gibbs oscillations (see Section 2.3.1).

### Localized Approximations

To localize Fourier series approximations over intervals, we multiply  $f$  by smooth windows that cover each of these intervals. The Balian-Low theorem (5.20) proves that one cannot build local Fourier bases with smooth windows of compact support. However, in Section 8.4.2 we construct orthonormal bases by replacing complex exponentials by cosine functions. For appropriate windows  $g_p$  of compact support  $[a_p - \eta_p, a_{p+1} + \eta_{p+1}]$ , Corollary 8.1 constructs an orthonormal basis of  $\mathbf{L}^2(\mathbb{R})$ :

$$\left\{ g_{p,k}(t) = g_p(t) \sqrt{\frac{2}{l_p}} \cos \left[ \pi \left( k + \frac{1}{2} \right) \frac{t - a_p}{l_p} \right] \right\}_{k \in \mathbb{N}, p \in \mathbb{Z}}.$$

**FIGURE 9.1**

**(a)** Original signal  $f$ . **(b)** Signal  $f_N$  approximated from  $N = 128$  lower-frequency Fourier coefficients with  $\|f - f_N\|/\|f\| = 8.63 \cdot 10^{-2}$ . **(c)** Signal  $f_N$  approximated from larger-scale Daubechies 4 wavelet coefficients with  $N = 128$  and  $\|f - f_N\|/\|f\| = 8.58 \cdot 10^{-2}$ .

Writing  $f$  in this local cosine basis is equivalent to segmenting it into several windowed components  $f_p(t) = f(t)g_p(t)$ , which are decomposed in a cosine IV basis. If  $g_p$  is  $C^\infty$ , the regularity of  $g_p(t)f(t)$  is the same as the regularity of  $f$  over  $[a_p - \eta_p, a_{p+1} + \eta_{p+1}]$ . Section 8.3.2 relates cosine IV coefficients to Fourier series coefficients. It follows from Theorem 9.2 that if  $f_p \in W^s(\mathbb{R})$ , then the approximation

$$f_{p,N} = \sum_{k=0}^{N-1} \langle f, g_{p,k} \rangle g_{p,k}$$

yields an error of

$$\varepsilon_l(N, f_p) = \|f_p - f_{p,N}\|^2 = o(N^{-2s}).$$

Thus, the approximation error in a local cosine basis depends on the local regularity of  $f$  over each window support.

### 9.1.3 Multiresolution Approximation Errors with Wavelets

Wavelets are constructed as bases of orthogonal complements of multiresolution approximation spaces. Thus, the projection error on multiresolution approximation spaces depends on the decay of wavelet coefficients. Linear approximations with wavelets behave essentially like Fourier approximations but with a better treatment of boundaries. They are also asymptotically optimal for uniformly regular signals. The linear error decay is computed for Sobolev differentiable functions and for uniformly Lipschitz  $\alpha$  functions.

#### Uniform Approximation Grid

Section 7.5 constructs multiresolution approximation spaces  $\mathbf{U}_N = \mathbf{V}_L$  of  $\mathbf{L}^2[0, 1]$  with their orthonormal basis of  $N = 2^{-L}$  scaling functions  $\{\phi_{L,n}(t)\}_{0 \leq n < 2^{-L}}$ . These scaling functions  $\phi_{L,n}(t) = \phi_L(t - 2^L n)$  with  $\phi_L(t) = 2^{-L/2}\phi(2^{-L}t)$  are finite elements translated over a uniform grid, modified near 0 and 1 so that their support remains in  $[0, 1]$ . The resulting projection of  $f$  in such a space is

$$f_N = P_{\mathbf{V}_L} f = \sum_{n=0}^{2^{-L}-1} \langle f, \phi_{L,n} \rangle \phi_{L,n}, \quad (9.12)$$

and

$$\langle f, \phi_{L,n} \rangle = \int f(t) \phi_L(t - 2^L n) dt = f \star \bar{\phi}_L(ns) \quad \text{with} \quad \bar{\phi}_L(t) = \phi_L(-t).$$

A different orthogonal basis of  $\mathbf{V}_L$  is obtained from wavelets at scales  $2^j > 2^L$  and scaling functions at a large scale  $2^J$ :

$$\left[ \{\phi_{J,n}\}_{0 \leq n < 2^{-J}}, \{\psi_{J,n}\}_{-J < j \leq J, 0 \leq n < 2^{-j}} \right]. \quad (9.13)$$

The approximation (9.12) can also be written as a wavelet approximation:

$$f_N = P_{\mathbf{V}_L} f = \sum_{j=L+1}^J \sum_{n=0}^{2^{-j}-1} \langle f, \psi_{j,n} \rangle \psi_{j,n} + \sum_{n=0}^{2^{-J}-1} \langle f, \phi_{J,n} \rangle \phi_{J,n}. \quad (9.14)$$

Since wavelets define an orthonormal basis of  $\mathbf{L}^2[0, 1]$ ,

$$\left[ \{\phi_{J,n}\}_{0 \leq n < 2^{-J}}, \{\psi_{J,n}\}_{-\infty < j \leq J, 0 \leq n < 2^{-j}} \right], \quad (9.15)$$

the approximation error is the energy of wavelet coefficients at scales smaller than  $2^L$ :

$$\varepsilon_l(N, f) = \|f - f_N\|^2 = \sum_{j=-\infty}^L \sum_{n=0}^{2^{-j}-1} |\langle f, \psi_{j,n} \rangle|^2. \quad (9.16)$$

In the following we suppose that wavelets  $\psi_{j,n}$  are  $\mathbf{C}^q$  ( $q$  times differentiable) and have  $q$  vanishing moments. The treatment of boundaries is the key difference

with Fourier approximations. Fourier approximations consider that the signal is periodic and if  $f(0) \neq f(1)$ , then the approximation of  $f$  behaves as if  $f$  was discontinuous. The periodic orthogonal wavelet bases in Section 7.5.1 do essentially the same. To improve this result, wavelets at the boundaries must keep their  $q$  vanishing moments, which requires us to modify them near the boundaries so that their supports remain in  $[0, 1]$ . Section 7.5.3 constructs such wavelet bases. They take advantage of the regularity of  $f$  over  $[0, 1]$  with no condition on  $f(0)$  and  $f(1)$ . For mathematical analysis, we only use these wavelets, without explicitly writing their shape modifications at the boundaries, to simplify notations. In numerical experiments, the folding boundary solution of Section 7.5.2 is more often used because it has a simpler algorithmic implementation. Folded wavelets have one vanishing moment at the boundary, which is often sufficient in applications.

### **Approximation Error versus Sobolev Regularity**

Like a Fourier basis, a wavelet basis provides an efficient approximation of uniformly regular signals. The decay of wavelet linear approximation errors is first related to the differentiability in the sense of Sobolev. Let  $\mathbf{W}^s[0, 1]$  be the Sobolev space of functions that are restrictions over  $[0, 1]$  of  $s$  times differentiable Sobolev function  $\mathbf{W}^s(\mathbb{R})$  defined over  $\mathbb{R}$ . If  $\psi$  has  $q$  vanishing moments, then (6.11) proves that the wavelet transform is a multiscale differential operator of order  $q$  at least. To test the differentiability of  $f$  up to order  $s$ , we need  $q > s$ . Theorem 9.4 gives a necessary and sufficient condition on wavelet coefficients so that  $f \in \mathbf{W}^s[0, 1]$ .

**Theorem 9.4.** Let  $0 < s < q$  be a Sobolev exponent. A function  $f \in \mathbf{L}^2[0, 1]$  is in  $\mathbf{W}^s[0, 1]$  if and only if

$$\sum_{j=-\infty}^J \sum_{n=0}^{2^{-j}-1} 2^{-2sj} |\langle f, \psi_{j,n} \rangle|^2 < +\infty. \quad (9.17)$$

**Proof.** We give an intuitive justification but not a proof of this result. To simplify, we suppose that the support of  $f$  is included in  $(0, 1)$ . If we extend  $f$  by zeros outside  $[0, 1]$ , then  $f \in \mathbf{W}^s(\mathbb{R})$ , which means that

$$\int_{-\infty}^{+\infty} |\omega|^{2s} |\hat{f}(\omega)|^2 d\omega < +\infty. \quad (9.18)$$

The low-frequency part of this integral always remains finite because  $f \in \mathbf{L}^2(\mathbb{R})$ :

$$\int_{|\omega| \leqslant 2^{-J}\pi} |\omega|^{2s} |\hat{f}(\omega)|^2 d\omega \leqslant 2^{-2sJ} \pi^{2s} \int_{|\omega| \leqslant \pi} |\hat{f}(\omega)|^2 d\omega \leqslant 2^{-2sJ} \pi^{2s} \|f\|^2.$$

The energy of  $\hat{\psi}_{j,n}$  is essentially concentrated in the intervals,  $[-2^{-j}2\pi, -2^{-j}\pi] \cup [2^{-j}\pi, 2^{-j}2\pi]$ . As a consequence,

$$\sum_{n=0}^{2^{-j}-1} |\langle f, \psi_{j,n} \rangle|^2 \sim \int_{2^{-j}\pi \leqslant |\omega| \leqslant 2^{-j+1}\pi} |\hat{f}(\omega)|^2 d\omega.$$

Over this interval  $|\omega| \sim 2^{-j}$ , so

$$\sum_{n=0}^{2^{-j}-1} 2^{-2sj} |\langle f, \psi_{j,n} \rangle|^2 \sim \int_{2^{-j}\pi \leq |\omega| \leq 2^{-j+1}\pi} |\omega|^{2s} |\hat{f}(\omega)|^2 d\omega.$$

It follows that

$$\sum_{j=-\infty}^J \sum_{n=0}^{2^{-j}-1} 2^{-2sj} |\langle f, \psi_{j,n} \rangle|^2 \sim \int_{|\omega| \geq 2^{-J}\pi} |\omega|^{2s} |\hat{f}(\omega)|^2 d\omega,$$

which explains why (9.18) is equivalent to (9.17). ■

This theorem proves that the Sobolev regularity of  $f$  is equivalent to a fast decay of the wavelet coefficients  $|\langle f, \psi_{j,n} \rangle|$  when scale  $2^j$  decreases. If  $\psi$  has  $q$  vanishing moments but is not  $q$  times continuously differentiable, then  $f \in \mathbf{W}^s[0, 1]$  implies (9.17), but the opposite implication is not true. Theorem 9.5 uses the decay condition (9.17) to characterize the linear approximation error with  $N$  wavelets.

**Theorem 9.5.** Let  $0 < s < q$  be a Sobolev exponent. A function  $f \in \mathbf{L}^2[0, 1]$  is in  $\mathbf{W}^s[0, 1]$  if and only if

$$\sum_{N=1}^{+\infty} N^{2s} \frac{\varepsilon_l(N, f)}{N} < +\infty, \quad (9.19)$$

which implies  $\varepsilon_l(N, f) = o(N^{-2s})$ .

**Proof.** Let us write the wavelets  $\psi_{j,n} = g_m$  with  $m = 2^{-j} + n$ . One can verify that the Sobolev condition (9.17) is equivalent to

$$\sum_{m=0}^{+\infty} |m|^{2s} |\langle f, g_m \rangle|^2 < +\infty.$$

The proof ends by applying Theorem 9.1. ■

If the wavelet has  $q$  vanishing moments but is not  $q$  times continuously differentiable, then  $f \in \mathbf{W}^s[0, 1]$  implies (9.19) but the opposite implication is false. Theorem 9.5 proves that  $f \in \mathbf{W}^s[0, 1]$  if and only if the approximation error  $\varepsilon_l(N, f)$  decays slightly faster than  $N^{-2s}$ . The wavelet approximation error is of the same order as the Fourier approximation error calculated in (9.11). However, Fourier approximations impose that the support of  $f$  is strictly included in  $[0, 1]$ , whereas wavelet approximation does not impose this condition or any other boundary condition because of the finer wavelet treatment of boundaries previously explained.

### Lipschitz Regularity

A different measure of uniform regularity is provided by Lipschitz exponents, which compute the error of a local polynomial approximation. A function  $f$  is uniformly

Lipschitz  $\alpha$  over  $[0, 1]$  if there exists  $K > 0$ , such that for any  $v \in [0, 1]$ , one can find a polynomial  $p_v$  of degree  $\lfloor \alpha \rfloor$  such that

$$\forall t \in [0, 1], \quad |f(t) - p_v(t)| \leq K |t - v|^\alpha. \quad (9.20)$$

The infimum of the  $K$  that satisfy (9.20) is the *homogeneous* Hölder  $\alpha$  norm  $\|f\|_{\tilde{C}^\alpha}$ . The Hölder  $\alpha$  norm of  $f$  also imposes that  $f$  is bounded:

$$\|f\|_{C^\alpha} = \|f\|_{\tilde{C}^\alpha} + \|f\|_\infty. \quad (9.21)$$

Space  $C^\alpha[0, 1]$  of functions  $f$  such that  $\|f\|_{C^\alpha} < +\infty$  is called a Hölder space. Theorem 9.6 characterizes the decay of wavelet coefficients.

**Theorem 9.6.** There exists  $B \geq A > 0$  such that

$$A \|f\|_{\tilde{C}^\alpha} \leq \sup_{j \geq J, 0 \leq n < 2^{-j}} 2^{-j(\alpha+1/2)} |\langle f, \psi_{j,n} \rangle| \leq B \|f\|_{\tilde{C}^\alpha}. \quad (9.22)$$

**Proof.** The proof of the equivalence between uniform Lipschitz regularity and the coefficient decay of a continuous wavelet transform is given in Theorem 6.3. This theorem gives a nearly equivalent result in the context of orthonormal wavelet coefficients that correspond to a sampling of a continuous wavelet transform computed with the same mother wavelet. Thus, the theorem proof is an adaptation of the proof of Theorem 6.3. This is illustrated by proving the right inequality of (9.22).

If  $f$  is uniformly Lipschitz  $\alpha$  on the support of  $\psi_{j,n}$ , since  $\psi_{j,n}$  is orthogonal the polynomial  $p_{2^j n}$ , approximating  $f$  at  $v = 2^j n$  yields

$$|\langle f, \psi_{j,n} \rangle| = |\langle f - p_{2^j n}, \psi_{j,n} \rangle| \leq \|f\|_{\tilde{C}^\alpha} \int 2^{-j/2} |\psi(2^{-j}(t - 2^j n))| |t - 2^j n|^\alpha dt. \quad (9.23)$$

With a change of variable, we get

$$|\langle f, \psi_{j,n} \rangle| \leq \|f\|_{\tilde{C}^\alpha} 2^{j(\alpha+1/2)} \int |\psi(t)| |t|^\alpha dt,$$

which proves the right inequality of (9.22). Observe that we do not use the wavelet regularity in this proof.

The left inequality of (9.22) is proved by following the continuous wavelet transform theorem (6.3) steps and replacing integrals by discrete sums over the position and scale of orthogonal wavelets. The regularity of wavelets plays an important role as shown by the proof of Theorem 6.3. In this case, there is no boundary issue because wavelets are adapted to the interval  $[0, 1]$  and keep their vanishing moments at the boundaries. ■

Similar to Theorem 9.4 for Sobolev differentiability, this theorem proves that uniform Lipschitz regularity is characterized by the decay of orthogonal wavelet coefficients when the scale  $2^j$  decreases. Hölder and Sobolev spaces belong to the larger class of Besov spaces, defined in Section 9.2.3.

If  $\psi$  has  $q$  vanishing moments but is not  $q$  times continuously differentiable, then the proof of Theorem 9.6 shows that the right inequality of (9.22) is valid.

Theorem 9.7 derives the decay of linear approximation errors for wavelets having  $q$  vanishing moments but that are not necessarily  $\mathbf{C}^q$ .

**Theorem 9.7.** If  $f$  is uniformly Lipschitz  $0 < \alpha \leq q$  over  $[0, 1]$ , then  $\varepsilon_l(N, f) = O(\|f\|_{\tilde{\mathcal{C}}^\alpha}^2 N^{-2\alpha})$ .

**Proof.** Theorem 9.6 proves that

$$|\langle f, \psi_{j,n} \rangle| \leq B \|f\|_{\tilde{\mathcal{C}}^\alpha} 2^{j(\alpha+1/2)}. \quad (9.24)$$

There are  $2^{-j}$  wavelet coefficients at scale  $2^j$ , so there are  $2^{-k}$  wavelet coefficients at scales  $2^j > 2^k$ . The right inequality (9.22) implies that

$$\varepsilon_l(2^{-k}, f) = \sum_{j=-\infty}^k \sum_{n=0}^{2^{-j}-1} |\langle f, \psi_{j,n} \rangle|^2 \leq B^2 \sum_{j=-\infty}^k 2^{-j} 2^{j(2\alpha+1)} = \frac{B^2 \|f\|_{\tilde{\mathcal{C}}^\alpha}^2 2^{2\alpha k}}{1 - 2^{-2\alpha}}.$$

For  $k = -\lfloor \log_2 N \rfloor$ , we derive that  $\varepsilon_l(N, f) = O(\|f\|_{\tilde{\mathcal{C}}^\alpha}^2 2^{2\alpha k}) = O(\|f\|_{\tilde{\mathcal{C}}^\alpha}^2 N^{-2\alpha})$ . ■

### Discontinuity and Bounded Variation

If  $f$  is not uniformly regular, then linear wavelet approximations perform poorly. If  $f$  has a discontinuity in  $(0, 1)$ , then  $f \notin \mathbf{W}^s[0, 1]$  for  $s > 1/2$ , so Theorem 9.5 proves that we cannot have  $\varepsilon_l(N, f) = O(N^{-\alpha})$  for  $\alpha > 1$ .

If  $f$  has a bounded total variation norm  $\|f\|_V$ , then Theorem 9.14 will prove that wavelet approximation errors satisfy  $\varepsilon_l(N, f) = O(\|f\|_V^2 N^{-1})$ . The same Fourier approximation result was obtained in Theorem 9.3. If  $f = C \mathbf{1}_{[0,1/2]}$ , then one can verify that wavelet approximation gives  $\varepsilon_l(N, f) \sim \|f\|_V^2 N^{-1}$  (Exercise 9.10).

Figure 9.1 gives an example of a discontinuous signal with bounded variation that is approximated by its larger-scale wavelet coefficients. The largest-amplitude errors are in the neighborhood of singularities, where the scale should be refined. The relative approximation error  $\|f - f_N\|/\|f\| = 8.56 \cdot 10^{-2}$  is almost the same as in a Fourier basis.

#### 9.1.4 Karhunen-Loève Approximations

Suppose that signals are modeled as realizations of a random process  $F$ . We prove that the basis that minimizes the average linear approximation error is the Karhunen-Loève basis, which diagonalizes the covariance operator of  $F$ . To avoid the subtleties of diagonalizing an infinite dimensional operator, we consider signals of finite dimension  $P$ , which means that  $F[n]$  is a random vector of size  $P$ .

Section A.6 in the Appendix reviews the covariance properties of random vectors. If  $F[n]$  does not have a zero mean, we subtract the expected value  $E\{F[n]\}$  from  $F[n]$  to get a zero mean. The random vector  $F$  can be decomposed in an orthogonal basis  $\{g_m\}_{0 \leq m < P}$ :

$$F = \sum_{m=0}^{P-1} \langle F, g_m \rangle g_m.$$

Each coefficient

$$\langle F, g_m \rangle = \sum_{n=0}^{P-1} F[n] g_m^*[n]$$

is a random variable (see Section A.6 in the Appendix). The approximation from the first  $N$  vectors of the basis is the orthogonal projection on the space  $\mathbf{U}_N$  generated by these vectors:

$$F_N = \sum_{m=0}^{N-1} \langle F, g_m \rangle g_m.$$

The resulting mean-square error is

$$E\{\varepsilon_l(N, F)\} = E\left\{\|F - F_N\|^2\right\} = \sum_{m=N}^{P-1} E\{|\langle F, g_m \rangle|^2\}.$$

The error is related to the covariance of  $F$  defined by

$$R_F[n, m] = E\{F[n] F^*[m]\}.$$

Let  $K_F$  be the covariance operator represented by this matrix. It is symmetric and positive and is thus diagonalized in an orthogonal basis called a *Karhunen-Loève basis*. This basis is not unique if several eigenvalues are equal. Theorem 9.8 proves that a Karhunen-Loève basis is optimal for linear approximations.

**Theorem 9.8.** For all  $N \geq 1$ , the expected approximation error

$$E\{\varepsilon_l(N, F)\} = E\{\|F - F_N\|^2\} = \sum_{m=N}^{P-1} E\{|\langle F, g_m \rangle|^2\}$$

is minimum if and only if  $\{g_m\}_{0 \leq m < P}$  is a Karhunen-Loève basis that diagonalizes the covariance  $K_F$  of  $F$  with vectors indexed in decreasing eigenvalue order:

$$\langle K_F g_m, g_m \rangle \geq \langle K_F g_{m+1}, g_{m+1} \rangle \quad \text{for } 0 \leq m < P-1.$$

**Proof.** Let us first observe that

$$E\{\varepsilon_l(F, N)\} = \sum_{m=N}^{P-1} \langle K_F g_m, g_m \rangle, \tag{9.25}$$

because for any vector  $z[n]$ ,

$$\begin{aligned} E\{|\langle F, z \rangle|^2\} &= E\left\{\sum_{n=0}^{P-1} \sum_{m=0}^{P-1} F[n] F[m] z[n] z^*[m]\right\} \\ &= \sum_{n=0}^{P-1} \sum_{m=0}^{P-1} R_F[n, m] z[n] z^*[m] \\ &= \langle K_F z, z \rangle. \end{aligned}$$

We now prove that (9.25) is minimum if the basis diagonalizes  $K_F$ . Let us consider an arbitrary orthonormal basis  $\{h_m\}_{0 \leq m < P}$ . The trace  $\text{tr}(K_F)$  of  $K_F$  is independent of the basis:

$$\text{tr}(K_F) = \sum_{m=0}^{P-1} \langle K_F h_m, h_m \rangle.$$

Thus, the basis that minimizes  $\sum_{m=N}^{P-1} \langle K_F h_m, h_m \rangle$ , maximizes  $\sum_{m=0}^{N-1} \langle K_F h_m, h_m \rangle$ .

Let  $\{g_m\}_{0 \leq m < P}$  be a basis that diagonalizes  $K_F$ :

$$K_F g_m = \sigma_m^2 g_m \quad \text{with} \quad \sigma_m^2 \geq \sigma_{m+1}^2 \quad \text{for} \quad 0 \leq m < P-1.$$

The theorem is proved by verifying that for all  $N \geq 0$ ,

$$\sum_{m=0}^{N-1} \langle K_F h_m, h_m \rangle \leq \sum_{m=0}^{N-1} \langle K_F g_m, g_m \rangle = \sum_{m=0}^{N-1} \sigma_m^2.$$

To relate  $\langle K_F h_m, h_m \rangle$  to the eigenvalues  $\{\sigma_i^2\}_{0 \leq i < P}$ , we expand  $h_m$  in the basis  $\{g_i\}_{0 \leq i < P}$ :

$$\langle K_F h_m, h_m \rangle = \sum_{i=0}^{P-1} |\langle h_m, g_i \rangle|^2 \sigma_i^2. \quad (9.26)$$

Thus,

$$\sum_{m=0}^{N-1} \langle K_F h_m, h_m \rangle = \sum_{m=0}^{N-1} \sum_{i=0}^{P-1} |\langle h_m, g_i \rangle|^2 \sigma_i^2 = \sum_{i=0}^{P-1} q_i \sigma_i^2$$

with

$$0 \leq q_i = \sum_{m=0}^{N-1} |\langle h_m, g_i \rangle|^2 \leq 1 \quad \text{and} \quad \sum_{i=0}^{P-1} q_i = N.$$

We evaluate

$$\begin{aligned} \sum_{m=0}^{N-1} \langle K_F h_m, h_m \rangle - \sum_{i=0}^{N-1} \sigma_i^2 &= \sum_{i=0}^{P-1} q_i \sigma_i^2 - \sum_{i=0}^{N-1} \sigma_i^2 \\ &= \sum_{i=0}^{P-1} q_i \sigma_i^2 - \sum_{i=0}^{N-1} \sigma_i^2 + \sigma_{N-1}^2 \left( N - \sum_{i=0}^{P-1} q_i \right) \\ &= \sum_{i=0}^{N-1} (\sigma_i^2 - \sigma_{N-1}^2) (q_i - 1) + \sum_{i=N}^{P-1} q_i (\sigma_i^2 - \sigma_{N-1}^2). \end{aligned}$$

Since the eigenvalues are listed in order of decreasing amplitude, it follows that

$$\sum_{m=0}^{N-1} \langle K_F h_m, h_m \rangle - \sum_{m=0}^{N-1} \sigma_m^2 \leq 0.$$

Suppose that this last inequality is an equality. We finish the proof by showing that  $\{h_m\}_{0 \leq m < P}$  must be a Karhunen-Loëve basis. If  $i < N$ , then  $\sigma_i^2 \neq \sigma_{N-1}^2$  implies  $q_i = 1$ . If  $i \geq N$ , then  $\sigma_i^2 \neq \sigma_{N-1}^2$  implies  $q_i = 0$ . This is valid for all  $N \geq 0$  if  $\langle h_m, g_i \rangle \neq 0$  only when  $\sigma_i^2 = \sigma_m^2$ . This means that the change of basis is performed inside each eigenspace of  $K_F$ , so  $\{h_m\}_{0 \leq m < P}$  also diagonalizes  $K_F$ . ■

The eigenvectors  $g_m$  of the covariance matrix are called *principal components*. Theorem 9.8 proves that a Karhunen-Loëve basis yields the smallest expected linear error when approximating a class of signals by their projection on  $N$  orthogonal vectors.

Theorem 9.8 has a simple geometrical interpretation. The realizations of  $F$  define a cloud of points in  $\mathbb{C}^P$ . The density of this cloud specifies the probability distribution of  $F$ . The vectors  $g_m$  of the Karhunen-Loëve basis give the directions of the principal axes of the cloud. Large eigenvalues  $\sigma_m^2$  correspond to directions  $g_m$  along which the cloud is highly elongated. Theorem 9.8 proves that projecting the realizations of  $F$  on these principal components yields the smallest average error. If  $F$  is a Gaussian random vector, the probability density is uniform along ellipsoids with axes proportional to  $\sigma_m$  in the direction of  $g_m$ . Thus, these principal directions are truly the preferred directions of the process.

### Random-Shift Processes

If the process is not Gaussian, its probability distribution can have a complex geometry, and a linear approximation along the principal axes may not be efficient. As an example, we consider a random vector  $F[n]$  of size  $P$  that is a random-shift modulo  $P$  of a deterministic signal  $f[n]$  of zero mean,  $\sum_{n=0}^{P-1} f[n] = 0$ :

$$F[n] = f[(n - Q) \bmod P]. \quad (9.27)$$

Shift  $Q$  is an integer random variable with a probability distribution that is uniform on  $[0, P - 1]$ :

$$\Pr(Q = p) = \frac{1}{P} \quad \text{for } 0 \leq p < P.$$

This process has a zero mean:

$$E\{F[n]\} = \frac{1}{P} \sum_{p=0}^{P-1} f[(n - p) \bmod P] = 0,$$

and its covariance is

$$\begin{aligned} R_F[n, k] &= E\{F[n]F[k]\} = \frac{1}{P} \sum_{p=0}^{P-1} f[(n - p) \bmod P]f[(k - p) \bmod P] \\ &= \frac{1}{P} f \circledast \bar{f}[n - k] \quad \text{with} \quad \bar{f}[n] = f[-n]. \end{aligned} \quad (9.28)$$

Thus,  $R_F[n, k] = R_F[n - k]$  with

$$R_F[k] = \frac{1}{P} f \circledast \bar{f}[k].$$

Since  $R_F$  is  $P$  periodic,  $F$  is a circular stationary random vector, as defined in Section A.6 in the Appendix. The covariance operator  $K_F$  is a circular convolution with  $R_F$ , and is therefore diagonalized in the discrete Fourier Karhunen-Loève basis  $\{\frac{1}{\sqrt{P}} \exp\left(\frac{i2\pi mn}{P}\right)\}_{0 \leq m < P}$ . The eigenvalues are given by the Fourier transform of  $R_F$ :

$$\sigma_m^2 = \hat{R}_F[m] = \frac{1}{P} |\hat{f}[m]|^2. \quad (9.29)$$

Theorem 9.8 proves that a linear approximation yields a minimum error in this Fourier basis. To better understand this result, let us consider an extreme case where  $f[n] = \delta[n] - \delta[n - 1]$ . Theorem 9.8 guarantees that the Fourier Karhunen-Loève basis produces a smaller expected approximation error than does a canonical basis of Diracs  $\{g_m[n] = \delta[n - m]\}_{0 \leq m < P}$ . Indeed, we do not know a priori the abscissa of the nonzero coefficients of  $F$ , so there is no particular Dirac that is better adapted to perform the approximation. Since the Fourier vectors cover the whole support of  $F$ , they always absorb part of the signal energy:

$$E \left\{ \left| \left\langle F[n], \frac{1}{\sqrt{P}} \exp\left(\frac{i2\pi mn}{P}\right) \right\rangle \right|^2 \right\} = \hat{R}_F[m] = \frac{4}{P} \sin^2\left(\frac{\pi k}{P}\right).$$

Therefore, selecting  $N$  higher-frequency Fourier coefficients yields a better mean-square approximation than choosing a priori  $N$  Dirac vectors to perform the approximation.

The linear approximation of  $F$  in a Fourier basis is not efficient because all the eigenvalues  $\hat{R}_F[m]$  have the same order of magnitude. A simple nonlinear algorithm can improve this approximation. In a Dirac basis,  $F$  is exactly reproduced by selecting the two Diracs corresponding to the largest-amplitude coefficients having positions  $Q$  and  $Q - 1$  that depend on each realization of  $F$ . A nonlinear algorithm that selects the largest-amplitude coefficient for each realization of  $F$  is not efficient in a Fourier basis. Indeed, the realizations of  $F$  do not have their energy concentrated over a few large-amplitude Fourier coefficients. This example shows that when  $F$  is not a Gaussian process, a nonlinear approximation may be much more precise than a linear approximation, and the Karhunen-Loève basis is no longer optimal.

## 9.2 NONLINEAR APPROXIMATIONS

Digital images or sounds are signals discretized over spaces of a large dimension  $N$ , because linear approximation error has a slow decay. Digital camera images have  $N \geq 10^6$  pixels, whereas one second of a CD recording has  $N = 40 \cdot 10^3$  samples. Sparse signal representations are obtained by projecting such signals over less vectors selected adaptively in an orthonormal basis of discrete signals in  $\mathbb{C}^N$ . This is equivalent to performing a nonlinear approximation of the input analog signal in a basis of  $L^2[0, 1]$ .

Section 9.2.1 analyzes the properties of the resulting nonlinear approximation error. Sections 9.2.2 and 9.2.3 prove that nonlinear wavelet approximations are equivalent to adaptive grids, and can provide sparse representations of signals including singularities. Approximations of functions in Besov spaces and with bounded variations are studied in Section 9.2.3.

### 9.2.1 Nonlinear Approximation Error

The discretization of an input analog signal  $f$  computes  $N$  sample values  $\{\langle f, \phi_n \rangle\}_{0 \leq n < N}$  that specify the projection  $f_N$  of  $f$  over an approximation space  $\mathbf{U}_N$  of dimension  $N$ . A nonlinear approximation further approximates this projection over a basis providing a sparse representation.

Let  $\mathcal{B} = \{g_m\}_{m \in \mathbb{N}}$  be an orthonormal basis of  $\mathbf{L}^2[0, 1]$  or  $\mathbf{L}^2[0, 1]^2$ , with the first  $N$  vectors defining a basis of  $\mathbf{U}_N$ . The orthogonal projection in  $\mathbf{U}_N$  can be written as

$$f_N(x) = \sum_{m=0}^{N-1} \langle f, g_m \rangle g_m(x),$$

and the linear approximation error is

$$\|f - f_N\|^2 = \sum_{n=N}^{+\infty} |\langle f, g_m \rangle|^2.$$

Let us reproject  $f_N$  over a subset of  $M < N$  vectors  $\{g_m\}_{m \in \Lambda}$  with  $\Lambda \subset [0, N - 1]$ :

$$f_\Lambda(x) = \sum_{m \in \Lambda} \langle f, g_m \rangle g_m(x).$$

The approximation error is the sum of the remaining coefficients:

$$\|f_N - f_\Lambda\|^2 = \sum_{m \notin \Lambda} |\langle f, g_m \rangle|^2. \quad (9.30)$$

The approximation set that minimizes this error is the set  $\Lambda_T$  of  $M$  vectors corresponding to the largest inner-product amplitude  $|\langle f, g_m \rangle|$ , and thus above a threshold  $T$  that depends on  $M$ :

$$\Lambda_T = \{m : 0 \leq m < N, |\langle f, g_m \rangle| \geq T\} \quad \text{with} \quad |\Lambda_T| = M. \quad (9.31)$$

The minimum approximation error is the energy of coefficients below  $T$ :

$$\varepsilon_n(M, f) = \|f_N - f_{\Lambda_T}\|^2 = \sum_{m \notin \Lambda_T} |\langle f, g_m \rangle|^2.$$

In the following, we often write that  $f_M = f_{\Lambda_T}$  is the best  $M$ -term approximation.

The overall error is the sum of the linear error when projecting  $f$  on  $\mathbf{U}_N$  and the nonlinear approximation error:

$$\varepsilon_n(M, f) = \|f - f_M\|^2 = \|f - f_N\|^2 + \|f_N - f_M\|^2. \quad (9.32)$$

If  $N$  is large enough so that all coefficients above  $T$  are in the first  $N$ ,

$$T \geq \max_{|m| \geq N} |\langle f, g_m \rangle| \quad \text{and hence} \quad N > \arg \max_m \{|\langle f, g_m \rangle| \geq T\}, \quad (9.33)$$

then the  $M$  largest signal coefficients are among the first  $N$  and the nonlinear error (9.32) is the minimum error obtained from  $M$  coefficients chosen anywhere in the infinite basis  $\mathcal{B} = \{g_m\}_{m \in \mathbb{N}}$ . In this case, the linear approximation space  $\mathbf{U}_N$  and  $f_N$  do not play any explicit role in the error  $\varepsilon_n(M, f)$ . If  $|\langle f, g_m \rangle| \leq C m^{-\beta}$  for some  $\beta > 0$ , then we can choose  $N \geq C^\beta T^\beta$ . In the following, this condition is supposed to be satisfied.

### Discrete Numerical Computations

The linear approximation space  $\mathbf{U}_N$  is important for discrete computations. A nonlinear approximation  $f_{\Lambda_T}$  is computed by calculating the nonlinear approximation of the discretized signal  $a[n] = \langle f, \phi_n \rangle$  for  $0 \leq n < N$ , and performing a discrete-to-analog conversion.

Since both the discretization family  $\{\phi_n\}_{0 \leq n < N}$  and the approximation basis  $\{g_m\}_{0 \leq m < N}$  are orthonormal bases of  $\mathbf{U}_N$ ,  $\{h_m[n] = \langle g_m, \phi_n \rangle\}_{0 \leq m < N}$  is an orthonormal basis of  $\mathbb{C}^N$ . Analog signal inner products in  $L^2[0, 1]$  and their discretization in  $\mathbb{C}^N$  are then equal:

$$\langle a[n], h_m[n] \rangle = \langle f(x), g_m(x) \rangle \quad \text{for } 0 \leq m < N. \quad (9.34)$$

The nonlinear approximation of the signal  $a[n]$  in the basis  $\{h_m\}_{0 \leq m < N}$  of  $\mathbb{C}^N$  is

$$a_{\Lambda_T}[n] = \sum_{m \in \Lambda_T} \langle a, h_m \rangle h_m[n] \quad \text{with} \quad \Lambda_T = \{m : |\langle a, h_m \rangle| \geq T\}.$$

It results from (9.34) that the analog conversion of this discrete signal is the nonlinear analog approximation:

$$f_{\Lambda_T}(x) = \sum_{n=0}^{N-1} a_{\Lambda_T}[n] \phi_n(x) = \sum_{n=0}^{N-1} a_{\Lambda_T}[n] \phi_n(x) = \sum_{m \in \Lambda_T} \langle f, g_m \rangle g_m(x).$$

The number of operations to compute  $a_{\Lambda_T}$  is dominated by the number of operations to compute the  $N$  signal coefficients  $\{\langle a, h_m \rangle\}_{0 \leq m < N}$ , which takes  $O(N \log_2 N)$  operations in a discrete Fourier basis, and  $O(N)$  in a discrete wavelet basis. Thus, reducing  $N$  decreases the number of operations and does not affect the nonlinear approximation error, as long as (9.33) is satisfied. Given this equivalence between discrete and analog nonlinear approximations, we now concentrate on analog functions to relate this error to their regularity.

### Approximation Error

To evaluate the nonlinear approximation error  $\varepsilon_n(M, f)$ , the coefficients  $\{|\langle f, g_m \rangle|\}_{m \in \mathbb{N}}$  are sorted in decreasing order. Let  $f_{\mathcal{B}}^r[k] = \langle f, g_{m_k} \rangle$  be the coefficient of rank  $k$ :

$$|f_{\mathcal{B}}^r[k]| \geq |f_{\mathcal{B}}^r[k+1]| \quad \text{with} \quad k > 0.$$

The best  $M$ -term nonlinear approximation computed from the  $M$  largest coefficients is:

$$f_M = \sum_{k=1}^M f_B^r[k] g_{m_k}. \quad (9.35)$$

The resulting error is

$$\varepsilon_n(M, f) = \|f - f_M\|^2 = \sum_{k=M+1}^{+\infty} |f_B^r[k]|^2.$$

Theorem 9.9 relates the decay of this approximation error as  $M$  increases to the decay of  $|f_B^r[k]|$  as  $k$  increases.

**Theorem 9.9.** Let  $s > 1/2$ . If there exists  $C > 0$  such that  $|f_B^r[k]| \leq C k^{-s}$ , then

$$\varepsilon_n(M, f) \leq \frac{C^2}{2s-1} M^{1-2s}. \quad (9.36)$$

Conversely, if  $\varepsilon_n(M, f)$  satisfies (9.36), then

$$|f_B^r[k]| \leq \left(1 - \frac{1}{2s}\right)^{-s} C k^{-s}. \quad (9.37)$$

**Proof.** Since

$$\varepsilon_n(M, f) = \sum_{k=M+1}^{+\infty} |f_B^r[k]|^2 \leq C^2 \sum_{k=M+1}^{+\infty} k^{-2s},$$

and

$$\sum_{k=M+1}^{+\infty} k^{-2s} \leq \int_M^{+\infty} x^{-2s} dx = \frac{M^{1-2s}}{2s-1}, \quad (9.38)$$

we derive (9.36).

Conversely, let  $\alpha < 1$ ,

$$\varepsilon_n(\alpha M, f) \geq \sum_{k=\alpha M+1}^M |f_B^r[k]|^2 \geq (1-\alpha) M |f_B^r[M]|^2.$$

So if (9.36) is satisfied,

$$|f_B^r[M]|^2 \leq \frac{\varepsilon_n(\alpha M, f)}{1-\alpha} M^{-1} \leq \frac{C^2}{2s-1} \frac{\alpha^{1-2s}}{1-\alpha} M^{-2s}.$$

For  $\alpha = 1 - 1/(2s)$ , we get (9.37) for  $k = M$ . ■

### **L<sup>p</sup> Spaces**

Theorem 9.10 relates the decay of sorted inner products to their  $\ell^p$  norm

$$\|f\|_{\mathcal{B},p} = \left( \sum_{m=0}^{+\infty} |\langle f, g_m \rangle|^p \right)^{1/p}.$$

It derives a decay upper bound of the error  $\varepsilon_n(M, f)$ .

**Theorem 9.10.** Let  $p < 2$ . If  $\|f\|_{\mathcal{B},p} < +\infty$ , then

$$|f_{\mathcal{B}}^r[k]| \leq \|f\|_{\mathcal{B},p} k^{-1/p} \quad (9.39)$$

and  $\varepsilon_n(M, f) = o(M^{1-2/p})$ .

**Proof.** We prove (9.39) by observing that

$$\|f\|_{\mathcal{B},p}^p = \sum_{n=1}^{+\infty} |f_{\mathcal{B}}^r[n]|^p \geq \sum_{n=1}^k |f_{\mathcal{B}}^r[n]|^p \geq k |f_{\mathcal{B}}^r[k]|^p.$$

To show that  $\varepsilon_n(M, f) = o(M^{1-2/p})$ , we set

$$S[k] = \sum_{n=k}^{2k-1} |f_{\mathcal{B}}^r[n]|^p \geq k |f_{\mathcal{B}}^r[2k]|^p.$$

Thus,

$$\begin{aligned} \varepsilon_n(M, f) &= \sum_{k=M+1}^{+\infty} |f_{\mathcal{B}}^r[k]|^2 \leq \sum_{k=M+1}^{+\infty} S[k/2]^{2/p} (k/2)^{-2/p} \\ &\leq \sup_{k>M/2} |S[k]|^{2/p} \sum_{k=M+1}^{+\infty} (k/2)^{-2/p}. \end{aligned}$$

Since  $\|f\|_{\mathcal{B},p}^p = \sum_{n=1}^{+\infty} |f_{\mathcal{B}}^r[n]|^p < +\infty$ , it follows that  $\lim_{k \rightarrow +\infty} \sup_{k>M/2} |S[k]| = 0$ . Thus, we derive from (9.38) that  $\varepsilon_n(M, f) = o(M^{1-2/p})$ . ■

This theorem specifies spaces of functions that are well approximated by a few vectors of an orthogonal basis  $\mathcal{B}$ . We denote

$$\mathbf{B}_{\mathcal{B},p} = \left\{ f \in \mathbf{H} : \|f\|_{\mathcal{B},p} < +\infty \right\}. \quad (9.40)$$

If  $f \in \mathbf{B}_{\mathcal{B},p}$ , then Theorem 9.10 proves that  $\varepsilon_n(M, f) = o(M^{1-2/p})$ . This is called a *Jackson inequality* [20]. Conversely, if  $\varepsilon_n(M, f) = O(M^{1-2/p})$ , then the *Bernstein inequality* (9.37) for  $s = 1/p$  shows that  $f \in \mathbf{B}_{\mathcal{B},q}$  for any  $q > p$ . Section 9.2.3 studies the properties of spaces  $\mathbf{B}_{\mathcal{B},p}$  for wavelet bases.

### 9.2.2 Wavelet Adaptive Grids

A nonlinear approximation in a wavelet orthonormal basis keeps the largest-amplitude coefficients. We saw in Section 6.1.3 that these coefficients occur near singularities. Thus, wavelet nonlinear approximation defines an adaptive grid that refines the approximation scale in the neighborhood of the signal sharp transitions. Such approximations are particularly well adapted to piecewise regular signals. The precision of nonlinear wavelet approximation is also studied for bounded variation functions and more general Besov space functions [209].

We consider a wavelet basis adapted to  $\mathbf{L}^2[0, 1]$ , constructed in Section 7.5.3 with compactly supported wavelets that are  $\mathbf{C}^q$  with  $q$  vanishing moments:

$$\mathcal{B} = \left[ \{\phi_{j,n}\}_{0 \leq n < 2^{-j}}, \{\psi_{j,n}\}_{-\infty < j \leq L, 0 \leq n < 2^{-j}} \right].$$

To simplify notation, we write  $\phi_{j,n} = \psi_{j+1,n}$ .

If the analog signal  $f \in \mathbf{L}^2[0, 1]$  is approximated at the scale  $2^L$  with  $N = 2^{-L}$  samples  $\{\langle f, \phi_{L,n} \rangle\}_{0 \leq n < 2^{-L}}$ , then the corresponding  $N$  wavelet coefficients  $\{\langle f, \psi_{j,n} \rangle\}_{n,j>L}$  are computed with  $O(N)$  operations with the fast wavelet transform algorithm of Section 7.3.1. The best nonlinear approximation of  $f \in \mathbf{L}^2[0, 1]$  from  $M$  wavelet coefficients above  $T$  at scales  $2^j > 2^L$  is

$$f_M = \sum_{(j,n) \in \Lambda_T} \langle f, \psi_{j,n} \rangle \psi_{j,n} \quad \text{with} \quad \Lambda_T = \{(j, n) : j > L, |\langle f, \psi_{j,n} \rangle| \geq T\}.$$

The approximation error is  $\varepsilon_n(M, f) = \sum_{(j,n) \notin \Lambda_T} |\langle f, \psi_{j,n} \rangle|^2$ . Theorem 9.11 proves that if  $f$  is bounded, then for a sufficiently large  $N$  the approximation support  $\Lambda_T$  corresponds to all possible wavelet coefficients above  $T$ .

**Theorem 9.11.** If  $f$  is bounded, then all wavelets producing coefficients above  $T$  are in an approximation space  $\mathbf{V}_L$  of dimension  $N = 2^{-L} = O(\|f\|_\infty^2 T^{-2})$ .

**Proof.** If  $f$  is bounded, then

$$\begin{aligned} |\langle f, \psi_{j,n} \rangle| &= \left| \int_0^1 f(t) 2^{-j/2} \psi(2^{-j}t - n) dt \right| \\ &\leq 2^{j/2} \sup_t |f(t)| \int_0^1 |\psi(t)| dt = 2^{j/2} \|f\|_\infty \|\psi\|_1. \end{aligned} \tag{9.41}$$

So,  $|\langle f, \psi_{j,n} \rangle| \geq T$  implies that  $2^j \geq T^2 \|f\|_\infty^{-2} \|\psi\|_1^{-2}$ , which proves the theorem for  $2^L = T^2 \|f\|_\infty^{-2} \|\psi\|_1^{-2}$ . ■

This theorem shows that for bounded signals, if the discretization  $2^L$  is sufficiently small, then the nonlinear approximation error computed from the first  $N = 2^{-L}$  wavelet coefficients is equal to the approximation error obtained by selecting the  $M$  largest wavelet coefficients in the infinite-dimensional wavelet basis. In the following, we suppose that this condition is satisfied, and thus do not have to worry about the discretization scale.

### Piecewise Regular Signals

Piecewise regular signals define a first simple model where nonlinear wavelet approximations considerably outperform linear approximations. We consider signals with a finite number of singularities and that are uniformly regular between singularities. Theorem 9.12 characterizes the linear and nonlinear wavelet approximation error decay for such signals.

**Theorem 9.12.** If  $f$  has  $K$  discontinuities on  $[0, 1]$  and is uniformly Lipschitz  $\alpha$  between these discontinuities, with  $1/2 < \alpha < q$ , then

$$\varepsilon_l(M, f) = O(K \|f\|_{C^\alpha}^2 M^{-1}) \quad \text{and} \quad \varepsilon_n(M, f) = O(\|f\|_{C^\alpha}^2 M^{-2\alpha}). \quad (9.42)$$

**Proof.** We distinguish type I wavelets  $\psi_{j,n}$  for  $n \in I_j$ , with a support including a point where  $f$  is discontinuous, from type II wavelets for  $n \in II_j$ , with a support that is included in a domain where  $f$  is uniformly Lipschitz  $\alpha$ .

Let  $C$  be the support size of  $\psi$ . At a scale  $2^j$ , each wavelet  $\psi_{j,n}$  has a support of size  $C2^j$ , translated by  $2^j n$ . Thus, there are at most  $|I_j| \leq C K$  type I wavelets  $\psi_{j,n}$  with supports that include at least one of the  $K$  discontinuities of  $f$ . Since  $\|f\|_\infty \leq \|f\|_{C^\alpha}$ , (9.41) shows for  $\alpha = 0$  that there exists  $B_0$  such that  $|\langle f, \psi_{j,n} \rangle| \leq B_0 \|f\|_{C^\alpha} 2^{j/2}$ .

At fine scales  $2^j$ , there are much more type II wavelets  $n \in II_j$ , but this number  $|II_j|$  is smaller than the total number  $2^{-j}$  of wavelets at this scale. Since  $f$  is uniformly Lipschitz  $\alpha$  on the support of  $\psi_{j,n}$ , the right inequality of (9.22) proves that there exists  $B$  such that

$$|\langle f, \psi_{j,n} \rangle| \leq B \|f\|_{C^\alpha} 2^{j(\alpha+1/2)}. \quad (9.43)$$

This linear approximation error from  $M = 2^{-k}$  wavelets satisfies

$$\begin{aligned} \varepsilon_l(M, f) &= \sum_{j \leq k} \left( \sum_{n \in I_j} |\langle f, \psi_{j,n} \rangle|^2 + \sum_{n \in II_j} |\langle f, \psi_{j,n} \rangle|^2 \right) \\ &\leq \sum_{j \leq k} \left( C K B_0^2 \|f\|_{C^\alpha}^2 2^j + 2^{-j} B^2 \|f\|_{C^\alpha}^2 2^{(2\alpha+1)j} \right) \\ &\leq \|f\|_{C^\alpha}^2 2 C K B_0^2 2^k + \|f\|_{C^\alpha}^2 (1 - 2^{-2\alpha})^{-1} B^2 2^{2\alpha k}. \end{aligned}$$

This inequality proves that for  $\alpha > 1/2$  the error term of type I wavelets dominates, and  $\varepsilon_l(M, f) = O(\|f\|_{C^\alpha}^2 K M^{-1})$ .

To compute the nonlinear approximaton error  $\varepsilon(M, f)$ , we evaluate the decay of ordered wavelet coefficients. Let  $f_B^r[k] = \langle f, \psi_{jk, n_k} \rangle$  be the coefficient of rank  $k$ :  $|f_B^r[k]| \geq |f_B^r[k+1]|$  for  $k \geq 1$ . Let  $f_{B,I}^r[k]$  and  $f_{B,II}^r[k]$  be the values of the wavelet coefficient of rank  $k$  in the type I and type II wavelets.

For  $l > 0$ , there are at most  $l K C$  type I coefficients at scales  $2^j > 2^{-l}$  and type I wavelet coefficients satisfy  $|\langle f, \psi_{j,n} \rangle| \leq B_0 \|f\|_{C^\alpha} 2^{-l/2}$  at scales  $2^j \leq 2^{-l}$ . It results that

$$f_{B,I}^r[IKC] \leq B_0 \|f\|_{C^\alpha} 2^{-l/2},$$

so  $f_{B,I}^r[k] = O(\|f\|_{C^\alpha} 2^{-k/(2KC)})$  has an exponential decay.

For  $l \geq 0$ , there are at most  $2^l$  type II wavelet coefficients at scales  $2^j > 2^{-l}$ , and type II wavelet coefficients satisfy  $|\langle f, \psi_{j,n} \rangle| \leq B \|f\|_{C^\alpha} 2^{-l(\alpha+1/2)}$  at scales  $2^j \leq 2^{-l}$ . It results that

$$f_{B,II}^r[2^{-l}] \leq B \|f\|_{C^\alpha} 2^{-l(\alpha+1/2)}.$$

It follows that  $f_{B,II}^r[k] = O(\|f\|_{C^\alpha} k^{-\alpha-1/2})$  for all  $k > 0$ .

Since type I coefficients have a much faster decay than type II coefficients, putting them together gives  $f_B^r[k] = O(\|f\|_{C^\alpha} k^{-\alpha-1/2})$ . From the inequality (9.36) of Theorem 9.9, it results that  $\varepsilon_n(M, f) = O(\|f\|_{C^\alpha}^2 M^{-2\alpha})$ . ■

Although there are few large wavelet coefficients created by the potential  $K$  discontinuities, the theorem proof shows that the linear approximation error is dominated by these discontinuities. On the contrary, these few wavelet coefficients have a negligible impact on the nonlinear approximation error. Thus, it decays as if there were no such discontinuities and  $f$  was uniformly Lipschitz  $\alpha$  over its whole support.

### Adaptive Grids

The approximation  $f_M$  calculated from the  $M$  largest-amplitude wavelet coefficients can be interpreted as an adaptive grid approximation where the approximation scale is refined in the neighborhood of singularities.

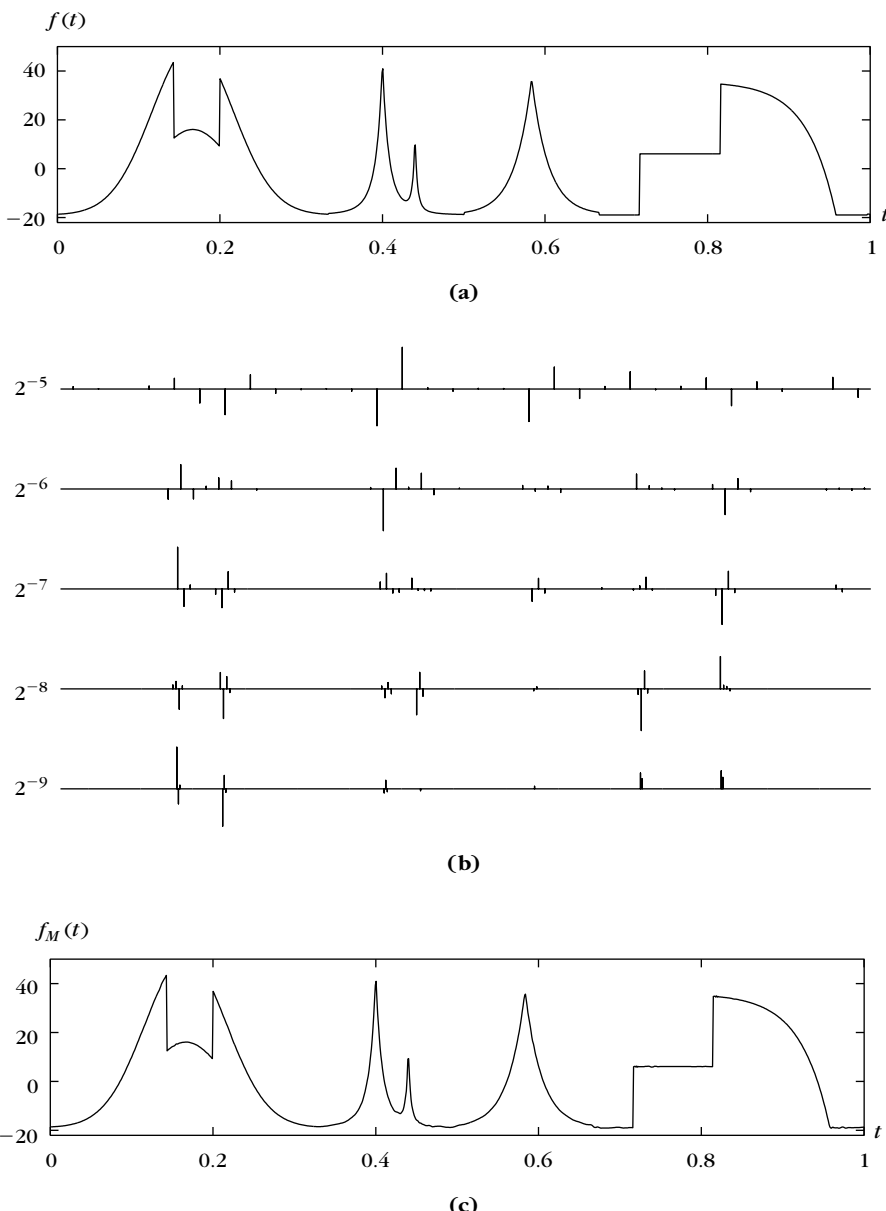
A nonlinear approximation keeps all coefficients above a threshold  $|\langle f, \psi_{j,n} \rangle| \geq T$ . In a region where  $f$  is uniformly Lipschitz  $\alpha$ , since  $|\langle f, \psi_{j,n} \rangle| \sim A 2^{j(\alpha+1/2)}$ , the coefficients above  $T$  are typically at scales

$$2^j > 2^l = \left(\frac{T}{A}\right)^{2/(2\alpha+1)}.$$

Setting all wavelet coefficients below the scale  $2^l$  to zero is equivalent to computing a local approximation of  $f$  at the scale  $2^l$ . The smaller the local Lipschitz regularity  $\alpha$ , the finer the approximation scale  $2^l$ .

Figure 9.2 shows the nonlinear wavelet approximation of a piecewise regular signal. Up and down Diracs correspond to positive and negative wavelet coefficients with an amplitude above  $T$ . The largest-amplitude wavelet coefficients are in the cone of influence of each singularity. The scale-space approximation support  $\Lambda_T$  specifies the geometry of the signal-sharp transitions. Since the approximation scale is refined in the neighborhood of each singularity, they are much better restored than in the fixed-scale linear approximation shown in Figure 9.1. The nonlinear approximation error in this case is 17 times smaller than the linear approximation error.

Nonlinear wavelet approximations are nearly optimal compared to adaptive spline approximations. A spline approximation  $\tilde{f}_M$  is calculated by choosing  $K$  nodes  $t_1 < t_2 < \dots < t_K$  inside  $[0, 1]$ . Over each interval  $[t_k, t_{k+1}]$ ,  $f$  is approximated by the closest polynomial of degree  $r$ . This polynomial spline  $\tilde{f}_M$  is specified by  $M = K(r+2)$  parameters, which are the node locations  $\{t_k\}_{1 \leq k \leq K}$  plus the  $K(r+1)$  parameters of the  $K$  polynomials of degree  $r$ . To reduce  $\|f - \tilde{f}_M\|$ , the nodes must be closely spaced when  $f$  is irregular and farther apart when  $f$  is smooth. However, finding the  $M$  parameters that minimize  $\|f - \tilde{f}_M\|$  is a difficult nonlinear optimization.

**FIGURE 9.2**

**(a)** Original signal  $f$ . **(b)** Each Dirac corresponds to one of the largest  $M = 0.15 N$  wavelet coefficients, calculated with a symmlet 4. **(c)** Nonlinear approximation  $f_M$  recovered from the  $M$  largest wavelet coefficients shown in (b),  $\|f - f_M\|/\|f\| = 5.1 \cdot 10^{-3}$ .

A spline wavelet basis of Battle-Lemarié gives nonlinear approximations that are also spline functions, but nodes  $t_k$  are restricted to dyadic locations  $2^j n$  with a scale  $2^j$  that is locally adapted to the signal regularity. It is computed with  $O(N)$  operations by projecting the signal in an approximation space of dimension  $N = O(T^2)$ . For large classes of signals, including balls of Besov spaces, the maximum approximation errors with wavelets or with optimized splines have the same decay rate when  $M$  increases [210]. Therefore, the computational overhead of an optimized spline approximation is not worth it.

### 9.2.3 Approximations in Besov and Bounded Variation Spaces

Studying the performance of nonlinear wavelet approximations more precisely requires introducing new spaces. As previously, we write the coarse-scale scaling functions  $\phi_{J,n} = \psi_{J+1,n}$ . The *Besov* space  $\mathbf{B}_{\beta,\gamma}^s[0, 1]$  is the set of functions  $f \in \mathbf{L}^2[0, 1]$  such that

$$\|f\|_{s,\beta,\gamma} = \left( \sum_{j=-\infty}^{J+1} \left[ 2^{-j(s+1/2-1/\beta)} \left( \sum_{n=0}^{2^{-j}-1} |\langle f, \psi_{j,n} \rangle|^{\beta} \right)^{1/\beta} \right]^{\gamma} \right)^{1/\gamma} < +\infty. \quad (9.44)$$

Frazier, Jawerth [260], and Meyer [375] proved that  $\mathbf{B}_{\beta,\gamma}^s[0, 1]$  does not depend on the particular choice of wavelet basis, as long as the wavelets in the basis have  $q > s$  vanishing moments and are in  $\mathbf{C}^q$ . Space  $\mathbf{B}_{\beta,\gamma}^s[0, 1]$  corresponds typically to functions that have a “derivative of order  $s$ ” that is in  $\mathbf{L}^\beta[0, 1]$ . The index  $\gamma$  is a fine-tuning parameter, which is less important. We need  $q > s$ , because a wavelet with  $q$  vanishing moments can test the differentiability of a signal only up to the order  $q$ . When removing the coarsest-scale scaling functions  $\phi_{J,n} = \psi_{J+1,n}$  from (9.44), the norm  $\|f\|_{s,\beta,\gamma}$  is called an homogeneous Besov norm that we shall write as  $\|f\|_{s,\beta,\gamma}^*$  and the corresponding homogeneous Besov space is  $\tilde{\mathbf{B}}_{\beta,\gamma}^s[0, 1]$ .

If  $\beta \geq 2$ , then functions in  $\mathbf{B}_{\beta,\gamma}^s[0, 1]$  have a uniform regularity of order  $s$ . For  $\beta = \gamma = 2$ , Theorem 9.4 proves that  $\mathbf{B}_{2,2}^s[0, 1] = \mathbf{W}^s[0, 1]$  is the space of  $s$  times differentiable functions in the sense of Sobolev. Theorem 9.5 proves that this space is characterized by the decay of the linear approximation error  $\varepsilon_l(N, f)$  and that  $\varepsilon_l(N, f) = o(N^{-2s})$ . Since  $\varepsilon_n(M, f) \leq \varepsilon_l(M, f)$ , clearly  $\varepsilon_n(M, f) = o(M^{-2s})$ . One can verify (Exercise 9.11) that nonlinear approximations do not improve linear approximations over Sobolev spaces. For  $\beta = \gamma = \infty$ , Theorem 9.6 proves that the homogeneous Besov norm is an homogeneous Hölder norm

$$\|f\|_{s,\infty,\infty}^* = \sup_{j \geq J,n} 2^{-j(\alpha+1/2)} |\langle f, \psi_{j,n} \rangle| \sim \|f\|_{\tilde{\mathbf{C}}^s}, \quad (9.45)$$

and the corresponding space  $\tilde{\mathbf{B}}_{\infty,\infty}^s[0, 1]$  is the homogeneous Hölder space of functions that are uniformly Lipschitz  $s$  on  $[0, 1]$ .

For  $\beta < 2$ , functions in  $\mathbf{B}_{\beta,\gamma}^s[0, 1]$  are not necessarily uniformly regular. Therefore, the adaptivity of nonlinear approximations significantly improves the decay rate of

the error. In particular, if  $p = \beta = \gamma$  and  $s = 1/2 + 1/p$ , then the Besov norm is a simple  $\ell^p$  norm:

$$\|f\|_{s,\beta,\gamma} = \left( \sum_{j=-\infty}^{J+1} \sum_{n=0}^{2^{-j}-1} |\langle f, \psi_{j,n} \rangle|^p \right)^{1/p}.$$

Theorem 9.10 proves that if  $f \in \mathbf{B}_{\beta,\gamma}^s[0, 1]$ , then  $\varepsilon_n(M, f) = o(M^{1-2/p})$ . The smaller  $p$  is, the faster the error decay. The proof of Theorem 9.12 shows that although  $f$  may be discontinuous, if the number of discontinuities is finite and if  $f$  is uniformly Lipschitz  $\alpha$  between these discontinuities, then its sorted wavelet coefficients satisfy  $|f'_B[k]| = O(k^{-\alpha-1/2})$ , so  $f \in \mathbf{B}_{\beta,\gamma}^s[0, 1]$  for  $1/p < \alpha + 1/2$ . This shows that these spaces include functions that are not  $s$  times differentiable at all points. The linear approximation error  $\varepsilon_l(M, f)$  for  $f \in \mathbf{B}_{\beta,\gamma}^s[0, 1]$  can decrease arbitrarily slowly because the  $M$  wavelet coefficients at the largest scales may be arbitrarily small. A nonlinear approximation is much more efficient in these spaces.

### Bounded Variation

Bounded variation functions are important examples of signals for which a nonlinear approximation yields a much smaller error than a linear approximation. The total variation norm is defined in (2.57) by

$$\|f\|_V = \int_0^1 |f'(t)| dt.$$

The derivative  $f'$  must be understood in the sense of distributions in order to include discontinuous functions. To compute the linear and nonlinear wavelet approximation error for bounded variation signals, Theorem 9.13 computes an upper and a lower bound of  $\|f\|_V$  from the modulus of wavelet coefficients.

**Theorem 9.13.** Consider a wavelet basis constructed with  $\psi$  such that  $\|\psi\|_V < +\infty$ . There exist  $A, B > 0$  such that for all  $f \in \mathbf{L}^2[0, 1]$ ,

$$\|f\|_V \leq B \sum_{j=-\infty}^{J+1} \sum_{n=0}^{2^{-j}-1} 2^{-j/2} |\langle f, \psi_{j,n} \rangle| = B \|f\|_{1,1,1}, \quad (9.46)$$

and

$$\|f\|_V \geq A \sup_{j \leq J} \left( \sum_{n=0}^{2^{-j}-1} 2^{-j/2} |\langle f, \psi_{j,n} \rangle| \right) = A \|f\|_{1,1,\infty}^*. \quad (9.47)$$

**Proof.** By decomposing  $f$  in the wavelet basis

$$f = \sum_{j=-\infty}^J \sum_{n=0}^{2^{-j}-1} \langle f, \psi_{j,n} \rangle \psi_{j,n} + \sum_{n=0}^{2^{-J}-1} \langle f, \phi_{J,n} \rangle \phi_{J,n}$$

we get

$$\|f\|_V \leq \sum_{j=-\infty}^J \sum_{n=0}^{2^{-j}-1} |\langle f, \psi_{j,n} \rangle| \|\psi_{j,n}\|_V + \sum_{n=0}^{2^{-J}-1} |\langle f, \phi_{J,n} \rangle| \|\phi_{J,n}\|_V. \quad (9.48)$$

The wavelet basis includes wavelets, with supports that are inside  $(0, 1)$ , and border wavelets, which are obtained by dilating and translating a finite number of mother wavelets. To simplify notations we write the basis as if there were a single mother wavelet:  $\psi_{j,n}(t) = 2^{-J/2}\psi(2^{-j}t - n)$ . Thus, we verify with a change of variable that

$$\|\psi_{j,n}\|_V = \int_0^1 2^{-j/2} 2^{-j} |\psi'(2^{-j}t - n)| dt = 2^{-j/2} \|\psi\|_V.$$

Since  $\phi_{J,n}(t) = 2^{-J/2}\phi(2^{-J}t - n)$ , we also prove that  $\|\phi_{J,n}\|_V = 2^{-J/2} \|\phi\|_V$ . Thus, the inequality (9.46) is derived from (9.48).

Since  $\psi$  has at least one vanishing moment, its primitive  $\theta$  is a function with the same support, which we suppose is included in  $[-K/2, K/2]$ . To prove (9.47) for  $j \leq J$ , we make an integration by parts:

$$\begin{aligned} \sum_{n=0}^{2^{-j}-1} |\langle f, \psi_{j,n} \rangle| &= \sum_{n=0}^{2^{-j}-1} \left| \int_0^1 f(t) 2^{-j/2} \psi(2^{-j}t - n) dt \right| \\ &= \sum_{n=0}^{2^{-j}-1} \left| \int_0^1 f'(t) 2^{j/2} \theta(2^{-j}t - n) dt \right| \\ &\leq 2^{j/2} \sum_{n=0}^{2^{-j}-1} \int_0^1 |f'(t)| |\theta(2^{-j}t - n)| dt. \end{aligned}$$

Since  $\theta$  has a support in  $[-K/2, K/2]$ ,

$$\sum_{n=0}^{2^{-j}-1} |\langle f, \psi_{j,n} \rangle| \leq 2^{j/2} K \sup_{t \in \mathbb{R}} |\theta(t)| \int_0^1 |f'(t)| dt \leq A^{-1} 2^{j/2} \|f\|_V. \quad (9.49)$$

This inequality proves (9.47). ■

This theorem shows that the total variation norm is bounded by two Besov norms:

$$A \|f\|_{1,1,\infty}^* \leq \|f\|_V \leq B \|f\|_{1,1,1}.$$

The lower bound is an homogeneous norm because the addition of a constant to  $f$  does not modify  $\|f\|_V$ . Space  $\mathbf{BV}[0, 1]$  of bounded variation functions is therefore embedded in the corresponding Besov spaces:

$$\mathbf{B}_{1,1}^1[0, 1] \subset \mathbf{BV}[0, 1] \subset B\mathbf{B}_{1,\infty}^1[0, 1].$$

Theorem 9.14 derives linear and nonlinear wavelet approximation errors for bounded variation signals.

**Theorem 9.14.** For all  $f \in \mathbf{BV}[0, 1]$  and  $M > 2q$ ,

$$\varepsilon_l(M, f) = O(\|f\|_V^2 M^{-1}), \quad (9.50)$$

and

$$\varepsilon_n(M, f) = O(\|f\|_V^2 M^{-2}). \quad (9.51)$$

**Proof.** Section 7.5.3 shows a wavelet basis of  $\mathbf{L}^2[0, 1]$  with boundary wavelets keeping their  $q$  vanishing moments that has  $2q$  different boundary wavelets and scaling functions, so the largest wavelet scale can be  $2^J = (2q)^{-1}$  but not smaller.

There are  $2^{-j}$  wavelet coefficients at a scale  $2^j$ , so for any  $L \leq J$ , there are  $2^{-L}$  wavelet and scaling coefficients at scales  $2^j > 2^L$ . The resulting linear wavelet approximation error is

$$\varepsilon_l(2^{-L}, f) = \sum_{j=-\infty}^L \sum_{n=0}^{2^{-j}-1} |\langle f, \psi_{j,n} \rangle|^2. \quad (9.52)$$

We showed in (9.47) that

$$\sum_{n=0}^{2^{-j}-1} |\langle f, \psi_{j,n} \rangle| \leq A^{-1} 2^{j/2} \|f\|_V,$$

and thus that

$$\sum_{n=0}^{2^{-j}-1} |\langle f, \psi_{j,n} \rangle|^2 \leq A^{-2} 2^j \|f\|_V^2.$$

It results from (9.52) that

$$\varepsilon_l(2^{-L}, f) \leq 2A^{-2} 2^L \|f\|_V^2.$$

Setting  $M = 2^{-L}$ , we derive (9.50).

Let us now prove the nonlinear approximation error bound (9.51). Let  $f_B^r[k]$  be the wavelet coefficient of rank  $k$ , excluding all the scaling coefficients  $\langle f, \phi_{J,n} \rangle$ , since we cannot control their value with  $\|f\|_V$ . We first show that there exists  $B_0$  such that for all  $f \in \mathbf{BV}[0, 1]$ ,

$$|f_B^r[k]| \leq B_0 \|f\|_V k^{-3/2}. \quad (9.53)$$

To take into account the fact that (9.53) does not apply to the  $2^J$  scaling coefficients  $\langle f, \phi_{J,n} \rangle$ , an upper bound of  $\varepsilon_n(M, f)$  is obtained by selecting the  $2^J$  scaling coefficients plus the  $M - 2^J$  biggest wavelet coefficients; thus,

$$\varepsilon_n(M, f) \leq \sum_{k=M-2^J+1}^{+\infty} |f_B^r[k]|^2. \quad (9.54)$$

For  $M > 2q = 2^{-J}$ , inserting (9.53) in (9.54) proves (9.51).

The upper bound (9.53) is proved by computing an upper bound of the number of coefficients larger than an arbitrary threshold  $T$ . At scale  $2^J$ , we denote by  $f_B^r[j, k]$

the coefficient of rank  $k$  among  $\{\langle f, \psi_{j,n} \rangle\}_{0 \leq n \leq 2^{-j}}$ . The inequality (9.49) proves that for all  $j \leq J$ ,

$$\sum_{n=0}^{2^{-j}-1} |\langle f, \psi_{j,n} \rangle| \leq A^{-1} 2^{j/2} \|f\|_V.$$

Thus, it follows from (9.39) that

$$|f_B^r[j, k]| \leq A^{-1} 2^{j/2} \|f\|_V k^{-1} = C 2^{j/2} k^{-1}.$$

Thus, at scale  $2^j$ , the number  $k_j$  of coefficients larger than  $T$  satisfies

$$k_j \leq \min(2^{-j}, 2^{j/2} C T^{-1}).$$

The total number  $k$  of coefficients larger than  $T$  is

$$\begin{aligned} k &= \sum_{j=-\infty}^J k_j \leq \sum_{2^j \geq (C^{-1}T)^{2/3}} 2^{-j} + \sum_{2^j > (C^{-1}T)^{2/3}} 2^{j/2} C T^{-1} \\ &\leq 6(C T^{-1})^{2/3}. \end{aligned}$$

By choosing  $T = |f_B^r[k]|$ , since  $C = A^{-1} \|f\|_V$ , we get

$$|f_B^r[k]| \leq 6^{3/2} A^{-1} \|f\|_V k^{-3/2},$$

which proves (9.53). ■

The asymptotic decay rate of linear and nonlinear approximation errors in Theorem 9.14 cannot be improved. If  $f \in \mathbf{BV}[0, 1]$  has discontinuities, then  $\varepsilon_l(M, f)$  decays like  $M^{-1}$  and  $\varepsilon_n(M, f)$  decays like  $M^{-2}$ . One can also prove [207] that this error-decay rate for all bounded variation functions cannot be improved by any type of nonlinear approximation scheme. In this sense, wavelets are optimal for approximating bounded variation functions.

### 9.3 SPARSE IMAGE REPRESENTATIONS

Approximation of images is more complex than one-dimensional signals, because singularities often belong to geometrical structures such as edges or textures. Nonlinear wavelet approximation defines adaptive approximation grids that are numerically highly effective. These approximations are optimal for bounded variation images, but not for images having edges that are geometrically regular. Section 9.3.2 introduces a piecewise regular image model with regular edges, and study adaptive triangulation approximations. Section 9.3.3 proves that curvelet frames yield asymptotically optimal approximation errors for such piecewise  $C^2$  regular images.

### 9.3.1 Wavelet Image Approximations

Linear and nonlinear approximations of functions in  $L^2[0, 1]^d$  can be calculated in separable wavelet bases. We concentrate on the two-dimensional case for image processing, and compute approximation errors for bounded variation images.

Section 7.7.4 constructs a separable wavelet basis of  $L^2[0, 1]^2$  from a wavelet basis of  $L^2[0, 1]$ , with separable products of wavelets and scaling functions. We suppose that all wavelets of the basis of  $L^2[0, 1]$  are  $C^q$  with  $q$  vanishing moments. The wavelet basis of  $L^2[0, 1]^2$  includes three mother wavelets  $\{\psi^l\}_{1 \leq l \leq 3}$  that are dilated by  $2^j$  and translated over a square grid of interval  $2^j$  in  $[0, 1]^2$ . As modulo modifications near the borders, these wavelets can be written as

$$\psi_{j,n}^l(x) = \frac{1}{2^j} \psi^l \left( \frac{x_1 - 2^j n_1}{2^j}, \frac{x_2 - 2^j n_2}{2^j} \right). \quad (9.55)$$

They have  $q$  vanishing moments in the sense that they are orthogonal to two-dimensional polynomials of a degree strictly smaller than  $q$ . If we limit the scales to  $2^j \leq 2^J$ , we must complete the wavelet family with two-dimensional scaling functions

$$\phi_{J,n}^2(x) = \frac{1}{2^J} \phi^2 \left( \frac{x_1 - 2^J n_1}{2^J}, \frac{x_2 - 2^J n_2}{2^J} \right)$$

to obtain the orthonormal basis of  $L^2[0, 1]^2$ :

$$\mathcal{B} = \left( \{\phi_{J,n}^2\}_{2^J n \in [0,1)^2} \cup \{\psi_{j,n}^l\}_{j \leq J, 2^j n \in [0,1)^2, 1 \leq l \leq 3} \right).$$

#### Linear Image Approximation

The linear discretization of an analog image in  $L^2[0, 1]^2$  can be defined by  $N = 2^{-2L}$  samples  $\{\langle f, \phi_{L,n}^2 \rangle\}_{2^L n \in [0,1)^2}$ , which characterize the orthogonal projection of  $f$  in the approximation space  $V_L$ . The precision of such linear approximations depends on the uniform image regularity.

Local image regularity can be measured with Lipschitz exponents. A function  $f$  is uniformly Lipschitz  $\alpha$  over a domain  $\Omega \subset \mathbb{R}^2$  if there exists  $K > 0$ , such that for any  $v \in \Omega$  one can find a polynomial  $p_v$  of degree  $\lfloor \alpha \rfloor$  such that

$$\forall x \in \Omega, \quad |f(x) - p_v(x)| \leq K |x - v|^\alpha. \quad (9.56)$$

The infimum of  $K$ , which satisfies (9.56), is the *homogeneous Hölder  $\alpha$  norm*  $\|f\|_{\tilde{C}^\alpha}$ . The Hölder  $\alpha$  norm of  $f$  also imposes that  $f$  is bounded:  $\|f\|_{C^\alpha} = \|f\|_{\tilde{C}^\alpha} + \|f\|_\infty$ . We write  $C^\alpha[0, 1]^2$  as the Hölder space of functions for which  $\|f\|_{C^\alpha} < +\infty$ . Similar to Theorem 9.15 in one dimension, Theorem 9.6 computes the linear approximation error decay of such functions, with  $C^q$  wavelets having  $q$  vanishing moments.

**Theorem 9.15.** There exists  $B \geq A > 0$  such that

$$A \|f\|_{\tilde{C}^\alpha} \leq \sup_{1 \leq l \leq 3, j \geq J, 0 \leq n < 2^{-j}} 2^{-j(\alpha+1)} |\langle f, \psi_{j,n}^l \rangle| \leq B \|f\|_{\tilde{C}^\alpha}. \quad (9.57)$$

**Proof.** The proof is essentially the same as the proof of Theorem 9.6 in one dimension. We shall only prove the right inequality. If  $f$  is uniformly Lipschitz  $\alpha$  on the support of  $\psi_{j,n}^l$ , since  $\psi_{j,n}^l$  is orthogonal to the polynomial  $p_{2^j n}$  approximating  $f$  at  $v = 2^j n$ , we get

$$\begin{aligned} |\langle f, \psi_{j,n}^l \rangle| &= |\langle f - p_{2^j n}, \psi_{j,n}^l \rangle| \leq \|f\|_{\tilde{\mathbf{C}}^\alpha} \int \int 2^{-j} |\psi^l(2^{-j}(x - 2^j n))| |x - 2^j n|^\alpha dx \\ &\leq \|f\|_{\tilde{\mathbf{C}}^\alpha} 2^{(\alpha+1)j} \int \int |\psi^l(x)| |x|^\alpha dx, \end{aligned}$$

which proves the right inequality of (9.57). The wavelet regularity is not used to prove this inequality. The left inequality requires that the wavelets are  $\mathbf{C}^q$ . ■

Theorem 9.16 computes the linear wavelet approximation error decay for images that are uniformly Lipschitz  $\alpha$ . It requires that wavelets have  $q$  vanishing moments, but no regularity condition is needed.

**Theorem 9.16.** If  $f$  is uniformly Lipschitz  $0 < \alpha \leq q$  over  $[0, 1]^2$ , then  $\varepsilon_l(N, f) = O(\|f\|_{\tilde{\mathbf{C}}^\alpha}^2 N^{-\alpha})$ .

**Proof.** There are  $3 2^{-2j}$  wavelet coefficients at scale  $2^j$  and  $2^{-2k}$  wavelet coefficients and scaling coefficients at scales  $2^j > 2^k$ . The right inequality of (9.57) proves that

$$|\langle f, \psi_{j,n}^l \rangle| \leq B \|f\|_{\tilde{\mathbf{C}}^\alpha} 2^{(\alpha+1)j}.$$

As a result,

$$\begin{aligned} \varepsilon_l(2^{-2k}, f) &= \sum_{j=-\infty}^k \sum_{l=1}^3 \sum_{2^j n \in [0, 1]^2} |\langle f, \psi_{j,n}^l \rangle|^2 \leq 3B^2 \|f\|_{\tilde{\mathbf{C}}^\alpha}^2 \sum_{j=-\infty}^k 2^{-2j} 2^{j(2\alpha+2)} \\ &= \frac{3B^2 \|f\|_{\tilde{\mathbf{C}}^\alpha}^2 2^{2\alpha k}}{1 - 2^{-2\alpha}}. \end{aligned}$$

For  $2k = -\lfloor \log_2 N \rfloor$ , we derive that  $\varepsilon_l(N, f) = O(\|f\|_{\tilde{\mathbf{C}}^\alpha}^2 2^{2\alpha k}) = O(\|f\|_{\tilde{\mathbf{C}}^\alpha}^2 N^{-\alpha})$ . ■

One can prove that this decay rate is optimal in the sense that no approximation scheme can improve decay rate  $N^{-\alpha}$  over all uniformly Lipschitz  $\alpha$  functions [20].

### NonLinear Approximation of Piecewise Regular Images

If an image has singularities, then linear wavelet approximations introduce large errors. In one dimension, an isolated discontinuity creates a constant number of large wavelet coefficients at each scale. As a result, nonlinear wavelet approximations are marginally influenced by a finite number of isolated singularities. Theorem 9.12 proves that if  $f$  is uniformly Lipschitz  $\alpha$  between these singularities, then the asymptotic error decay behaves as if there was no singularity. In two dimensions, if  $f$  is uniformly Lipschitz  $\alpha$ , then Theorem 9.16 proves that the linear approximation error from  $M$  wavelets satisfies  $\varepsilon_l(M, f) = O(M^{-\alpha})$ . Thus, we can

hope that piecewise regular images yield a nonlinear approximation error having the same asymptotic decay. Regretfully, this is wrong.

A piecewise regular image has discontinuities along curves of dimension 1, which create a nonnegligible number of high-amplitude wavelet coefficients. As a result, even though the function may be infinitely differentiable between discontinuities, the nonlinear approximation error  $\varepsilon_n(M, f)$  decays only like  $M^{-1}$ .

As an example, suppose that  $f = C \mathbf{1}_\Omega$  is the indicator function of a set  $\Omega$  the border  $\partial\Omega$  of which has a finite length, as shown in Figure 9.3. If the support of  $\psi_{j,n}^l$  does not intersect the border  $\partial\Omega$ , then  $\langle f, \psi_{j,n}^l \rangle = 0$  because  $f$  is constant over the support of  $\psi_{j,n}^l$ . The wavelets  $\psi_{j,n}^l$  have a square support of size proportional to  $2^j$ , which is translated on a grid of interval  $2^j$ . Since  $\partial\Omega$  has a finite length  $L$ , there are on the order of  $L 2^{-j}$  wavelets with supports that intersect  $\partial\Omega$ . Figure 9.3(b) illustrates the position of these coefficients.

Since  $f$  is bounded, the result from (9.57) for  $\alpha = 0$  is that  $|\langle f, \psi_{j,n}^l \rangle| = O(C 2^j)$ . Along the border, wavelet coefficients typically have an amplitude of  $|\langle f, \psi_{j,n}^l \rangle| \sim C 2^j$ . Thus, the  $M$  largest coefficients are typically at scales  $2^j \geq L/M$ . Selecting these  $M$  largest coefficients yields an error of

$$\varepsilon_n(M, f) \sim \sum_{j=-\infty}^{\log_2(L/M)-1} L 2^{-j} C^2 2^{2j} = (C L)^2 M^{-1}. \quad (9.58)$$

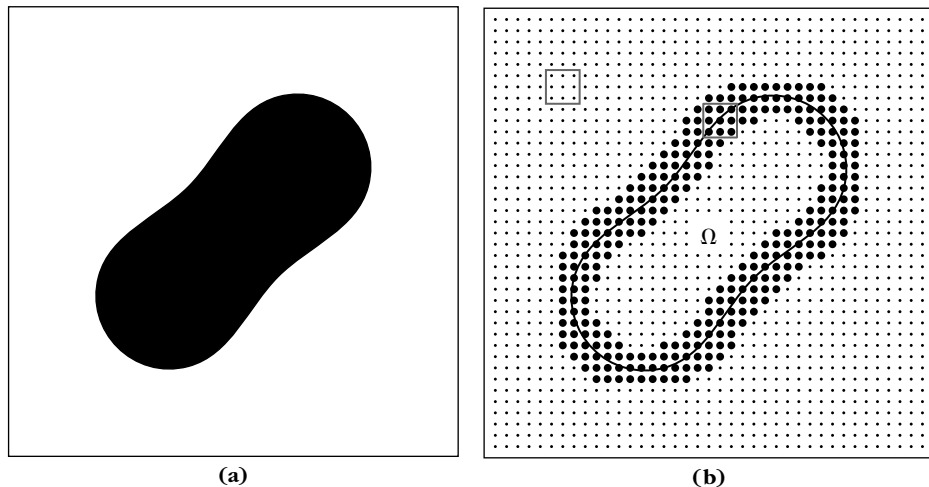


**FIGURE 9.3**

(a) Image  $f = \mathbf{1}_\Omega$ . (b) At the scale  $2^j$ , the wavelets  $\psi_{j,n}^l$  have a square support of width proportional to  $2^j$ . This support is translated on a grid of interval  $2^j$ , which is indicated by the smaller dots. The darker dots correspond to wavelets with support that intersect the frontier of  $\Omega$ , for which  $\langle f, \psi_{j,n}^l \rangle \neq 0$ .

Thus, the large number of wavelet coefficients produced by the edges of  $f$  limit the error decay to  $M^{-1}$ .

Two questions then arise. Is the class of images that have a wavelet approximation error that decays like  $M^{-1}$  sufficiently large enough to incorporate interesting image models? The following section proves that this class includes all bounded variation images. The second question is: Is it possible to find sparse signal representations that are better than wavelets to approximate images having regular edges  $z$ . We address this question in Section 9.3.2.

### Bounded Variation Images

Bounded variation functions provide good models for large classes of images that do not have irregular textures. The total variation of  $f$  is defined in Section 2.3.3 by

$$\|f\|_V = \int_0^1 \int_0^1 |\vec{\nabla} f(x)| dx. \quad (9.59)$$

The partial derivatives of  $\vec{\nabla} f$  must be taken in the general sense of distributions in order to include discontinuous functions. Let  $\partial\Omega_t$  be the level set defined as the boundary of

$$\Omega_t = \{x \in \mathbb{R}^2 : f(x) > t\}.$$

Theorem 2.9 proves that the total variation depends on length  $H^1(\partial\Omega_t)$  of level sets:

$$\int_0^1 \int_0^1 |\vec{\nabla} f(x)| dx = \int_{-\infty}^{+\infty} H^1(\partial\Omega_t) dt. \quad (9.60)$$

It results that if  $f = C \mathbf{1}_\Omega$ , then  $\|f\|_V = C L$  where  $L$  is the length of the boundary of  $\Omega$ . Thus, indicator functions of sets have a bounded total variation that is proportional to the length of their “edges.”

Linear and nonlinear approximation errors of bounded variation images are computed by evaluating the decay of their wavelet coefficients across scales. We denote with  $f_B^r[k]$  the rank  $k$  wavelet coefficient of  $f$ , without including the  $2^{2J}$  scaling coefficients  $\langle f, \phi_{J,n}^2 \rangle$ . Theorem 9.17 gives upper and lower bounds on  $\|f\|_V$  from wavelet coefficients. Wavelets are supposed to have a compact support and need only one vanishing moment.

**Theorem 9.17:** Cohen, DeVore, Pertrushev, Xu. There exist  $A, B_1, B_2 > 0$  such that if  $\|f\|_V < +\infty$ , then

$$\sum_{j=-\infty}^J \sum_{l=1}^3 \sum_{2^j n \in [0,1]^2} |\langle f, \psi_{j,n}^l \rangle| + \sum_{2^J n \in [0,1]^2} |\langle f, \phi_{J,n}^2 \rangle| \geq A \|f\|_V, \quad (9.61)$$

$$\sup_{\substack{-\infty < j \leq J \\ 1 \leq l \leq 3}} \left( \sum_{2^j n \in [0,1]^2} |\langle f, \psi_{j,n}^l \rangle| \right) \leq B_1 \|f\|_V, \quad (9.62)$$

and

$$|f_B^r[k]| \leq B_2 \|f\|_V k^{-1}. \quad (9.63)$$

**Proof.** In two dimensions, a wavelet total variation does not depend on scale and position.

Indeed, with a change of variable  $x' = 2^{-j}x - n$ , we get

$$\|\psi_{j,n}^l\|_V = \iint |\vec{\nabla} \psi_{j,n}^l(x)| dx = \iint |\vec{\nabla} \psi^l(x')| dx' = \|\psi^l\|_V.$$

Similarly,  $\|\phi_{j,n}^2\|_V = \|\phi^2\|_V$ . The inequalities (9.61) and (9.62) are proved with the same derivation steps as in Theorem 9.13 for one-dimensional bounded variation functions.

The proof of (9.63) is technical and can be found in [175]. The inequality (9.62) proves that wavelet coefficients have a bounded  $L^1$  norm at each scale  $2^j$ . It results from (9.39) in Theorem 9.10 that ranked wavelet coefficients at each scale  $2^j$  have a decay bounded by  $B_1 \|f\|_V k^{-1}$ . The inequality (9.63) is finer since it applies to the ranking of wavelet coefficients at all scales. ■

The Lena image is an example of finite-resolution approximation of a bounded variation image. Figure 9.4 shows that its sorted wavelet coefficients  $\log_2 |f_B^r[k]|$  decays with a slope that reaches  $-1$  as  $\log_2 k$  increases, which verifies that  $|f_B^r[k]| = O(k^{-1})$ . In contrast, the Mandrill image shown in Figure 10.7 does not have a bounded total variation because of the fur texture. As a consequence,  $\log_2 |f_B^r[k]|$  decays more slowly, in this case with a slope that reaches  $-0.65$ .

A function with finite total variation does not necessarily have a bounded amplitude, but images do have a bounded amplitude. Theorem 9.18 incorporates this hypothesis to compute linear approximation errors.

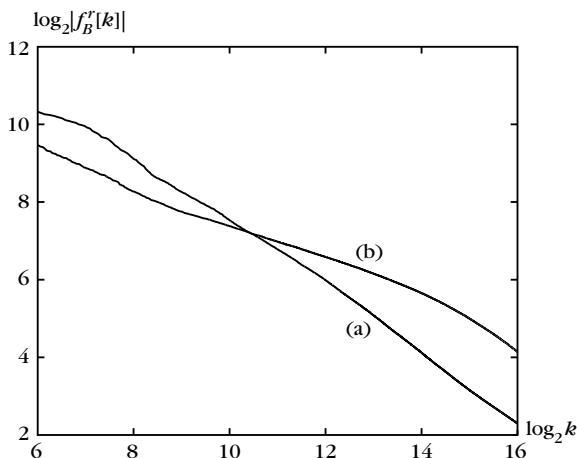


FIGURE 9.4

Sorted wavelet coefficients  $\log_2 |f_B^r[k]|$  as a function of  $\log_2 k$  for two images. (a) Lena image shown in Figure 9.5(a). (b) Mandrill image shown in Figure 10.7.

**Theorem 9.18.** If  $\|f\|_V < +\infty$  and  $\|f\|_\infty < +\infty$ , then

$$\varepsilon_l(M, f) = O(\|f\|_V \|f\|_\infty M^{-1/2}) \quad (9.64)$$

and

$$\varepsilon_n(M, f) = O(\|f\|_V^2 M^{-1}). \quad (9.65)$$

**Proof.** The linear approximation error from  $M = 2^{-2m}$  wavelets is

$$\varepsilon_l(2^{-2m}, f) = \sum_{j=-\infty}^m \sum_{l=1}^3 \sum_{2^j n \in [0, 1]^2} |\langle f, \psi_{j,n}^l \rangle|^2. \quad (9.66)$$

We shall verify that there exists  $B > 0$  such that for all  $j$  and  $l$ ,

$$\sum_{2^j n \in [0, 1]^2} |\langle f, \psi_{j,n}^l \rangle|^2 \leq B \|f\|_V \|f\|_\infty 2^j. \quad (9.67)$$

Applying this upper bound to the sum (9.66) proves that

$$\varepsilon_l(2^{-2m}, f) \leq 6B1 \|f\|_V \|f\|_\infty 2^m,$$

from which (9.64) is derived.

The upper bound (9.67) is calculated with (9.62), which shows that there exists  $B_2 > 0$  such that for all  $j$  and  $l$ ,

$$\sum_{2^j n \in [0, 1]^2} |\langle f, \psi_{j,n}^l \rangle| \leq B_2 \|f\|_V. \quad (9.68)$$

The amplitude of a wavelet coefficient can also be bounded:

$$|\langle f, \psi_{j,n}^l \rangle| \leq \|f\|_\infty \|\psi_{j,n}^l\|_1 = \|f\|_\infty 2^j \|\psi^l\|_1,$$

where  $\|\psi^l\|_1$  is the  $\mathbf{L}^1[0, 1]^2$  norm of  $\psi^l$ . If  $B_3 = \max_{1 \leq l \leq 3} \|\psi^l\|_1$ , this yields

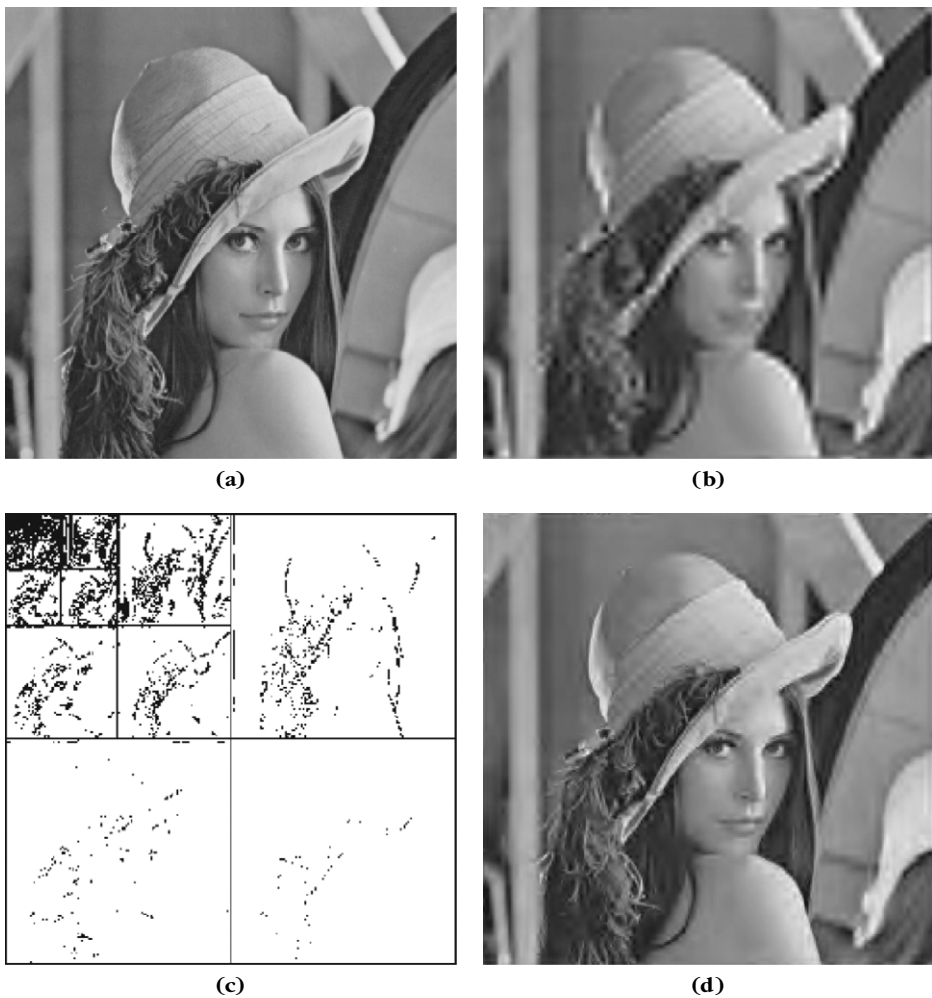
$$|\langle f, \psi_{j,n}^l \rangle| \leq B_3 2^j \|f\|_\infty. \quad (9.69)$$

Since  $\sum_n |a_n|^2 \leq \sup_n |a_n| \sum_n |a_n|$ , we get (9.67) from (9.68) and (9.69).

The nonlinear approximation error is a direct consequence of the sorted coefficient decay (9.63). It results from (9.63) and (9.36) that  $\varepsilon_n(M, f) = O(\|f\|_V^2 M^{-1})$ . ■

This theorem shows that nonlinear wavelet approximations of bounded variation images can yield much smaller errors than linear approximations. The decay bounds of this theorem are tight in the sense that one can find functions, for which  $\varepsilon_l(M, f)$  and  $\varepsilon_n(M, f)$  decay, respectively, like  $M^{-1/2}$  and  $M^{-1}$ . This is typically the case for bounded variation images including discontinuities along edges, for example,  $f = C \mathbf{1}_\Omega$ . The Lena image in Figure 9.5(a) is another example.

Figure 9.5(b) is a linear approximation calculated with  $M = N/16$  largest-scale wavelet coefficients. This approximation produces a uniform blur and creates Gibbs oscillations in the neighborhood of contours. Figure 9.5(c) gives the nonlinear

**FIGURE 9.5**

- (a) Lena image  $f$  of  $N = 256^2$  pixels. (b) Linear approximations  $f_M$  calculated from the  $M = N/16$  symmlet 4 wavelet coefficients at the largest scales:  $\|f - f_M\|/\|f\| = 0.036$ .  
 (c) The support of the  $M = N/16$  largest-amplitude wavelet coefficients are shown in black.  
 (d) Nonlinear approximation  $f_M$  calculated from the  $M$  largest-amplitude wavelet coefficients:  $\|f - f_M\|/\|f\| = 0.011$ .

approximation support  $\Lambda_T$  of  $M = N/16$  largest-scale wavelet coefficients. Large-amplitude coefficients are located where the image intensity varies sharply, in particular along the edges. The resulting nonlinear approximation is shown in Figure 9.5(d). The nonlinear approximation error is much smaller than the linear

approximation error— $\varepsilon_n(M, f) \leq \varepsilon_l(M, f)/10$ —and the image quality is indeed better. As in one dimension, this nonlinear wavelet approximation can be interpreted as an adaptive grid approximation, which refines the approximation resolution near edges and textures by keeping wavelet coefficients at smaller scales.

### 9.3.2 Geometric Image Models and Adaptive Triangulations

Bounded variation image models correspond to images that have level sets with a finite average length, but they do not imply any geometrical regularity of these level sets. The level sets and “edges” of many images such as Lena are often piecewise regular curves. This geometric regularity can be used to improve the sparsity of image representations.

When an image is uniformly Lipschitz  $\alpha$ , Theorem 9.16 proves that wavelet nonlinear approximations have an error  $\varepsilon_l(M, f) = O(M^{-\alpha})$ , which is optimal. However, as soon as the image is discontinuous along an edge, then the error decay rate drops to  $\varepsilon_n(M, f) = O(M^{-1})$ , because edges create a number of large wavelet coefficients that is proportional to their length. This decay rate is improved by representations taking advantage of edge geometric regularities. We introduce a piecewise regular image model that incorporates the geometric regularity of edges. Approximations of piecewise regular images are studied with adaptive triangulations.

#### Piecewise $C^\alpha$ Image Models

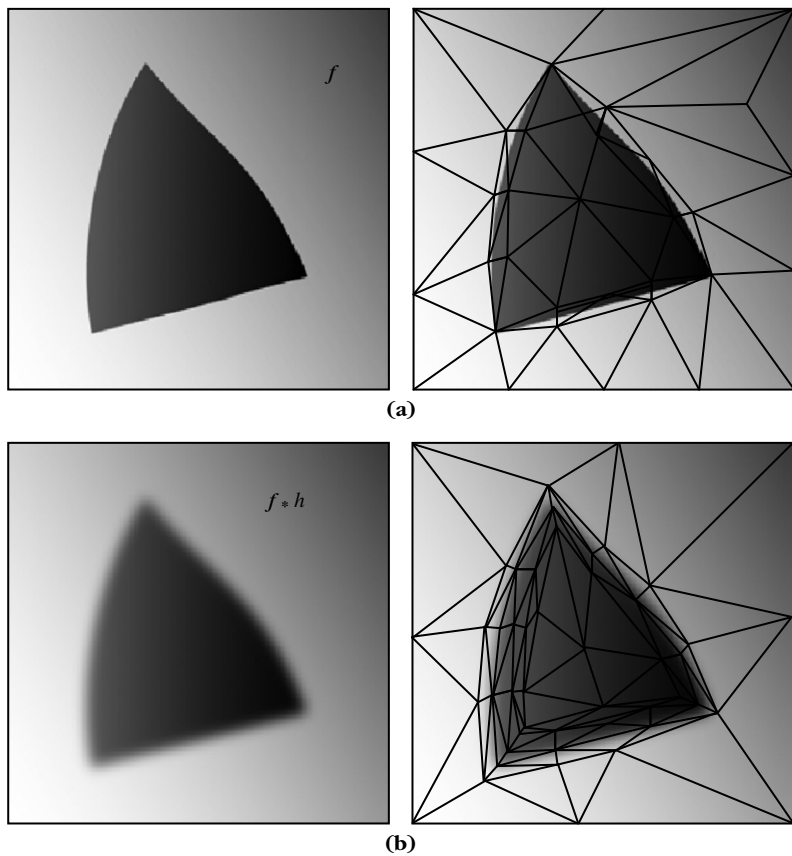
Piecewise regular image models include edges that are also piecewise regular. These edges are typically occlusion contours of objects in images. The regularity is measured in the sense of uniform Lipschitz regularity with Hölder norms  $\|f\|_{C^\alpha}$ , defined in (9.20) and (9.56) for one- and two-dimensional functions, respectively. Edges are supposed to be a finite union of curves  $e_k$  that are uniformly Lipschitz  $\alpha$  in  $[0, 1]^2$ ; between edges, the image is supposed to be uniformly Lipschitz  $\alpha$ . To model the blur introduced by the optics or by diffraction phenomena, the image model incorporates a convolution by an unknown regular kernel  $h_s$ , with scale  $s$  that is a parameter.

**Definition 9.1.** A function  $f \in L^2[0, 1]^2$  is said to be a piecewise  $C^\alpha$  with a blurring scale  $s \geq 0$ , if  $f = \bar{f} \star h_s$  where  $\bar{f}$  is uniformly Lipschitz  $\alpha$  on  $\Omega = [0, 1]^2 - \{e_k\}_{1 \leq k < K}$ . If  $s > 0$ , then  $h_s(x) = s^{-2}h(s^{-1}x)$  where  $h$  is a uniformly Lipschitz  $\alpha$  kernel with a support in  $[-1, 1]$ , and if  $s = 0$ , then  $h_0 = \delta$ . Curves  $e_k$  are uniformly Lipschitz  $\alpha$  and do not intersect tangentially.

When the blurring scale  $s = 0$ , then  $f = \bar{f} \star h_0 = \bar{f}$  is typically discontinuous along the edges. When  $s > 0$ , then  $\bar{f} \star h_s$  is blurred and discontinuities along edges are diffused on a neighborhood of size  $s$ , as shown in Figure 9.6.

#### Approximations with Adapted Triangulations

Wavelet approximations are inefficient to recover regular edges because it takes many wavelets to cover the edge at each scale, as shown by Figure 9.3. To improve

**FIGURE 9.6**

Adaptive triangulations for piecewise linear approximations of a piecewise  $\mathbf{C}^2$  image, without (a) and with (b) a blurring kernel.

this approximation, it is necessary to use elongated approximation elements. For  $\mathbf{C}^2$  piecewise regular images, it is proved that piecewise linear approximations over  $M$  adapted triangles can reach the optimal  $O(M^{-2})$  error decay, as if the image had no singularities.

For the solution of partial differential equations, the local optimization of anisotropic triangles was introduced by Babuška and Aziz [90]. Adaptive triangulations are indeed useful in numerical analysis, where shocks or boundary layers require anisotropic refinements of finite elements [77, 410, 434]. A planar triangulation  $(\mathcal{V}, \mathcal{T})$  of  $[0, 1]^2$  is composed of vertices  $\mathcal{V} = \{x_i\}_{0 \leq i < p}$  and disjoint triangular faces  $\mathcal{T} = \{T_k\}_{0 \leq k < M}$  that cover the image domain

$$\bigcup_{k=0}^{M-1} T_k = [0, 1]^2.$$

Let  $M$  be the number of triangles. We consider an image approximation  $\tilde{f}_M$  obtained with linear interpolations of the image values at the vertices. For each  $x_i \in \mathcal{V}$ ,  $\tilde{f}_M(x_i) = f(x_i)$ , and  $\tilde{f}_M(x)$  is linear on each triangular face  $T_k$ . A function  $f$  is well approximated with  $M$  triangles if the shapes of these triangles are optimized to capture the regularity of  $f$ .

Theorem 9.19 proves that adapted triangulations for piecewise  $C^2$  images leads to the optimal decay rate  $O(M^{-2})$  by sketching the construction of a well-adapted triangulation.

**Theorem 9.19.** If  $f$  is a piecewise  $C^2$  image, then there exists  $C$  such that for any  $M$  one can construct a triangulation  $(\mathcal{V}, \mathcal{T})$  with  $M$  triangles over which the piecewise linear interpolation  $\tilde{f}_M$  satisfies

$$\|f - \tilde{f}_M\|^2 \leq CM^{-2}. \quad (9.70)$$

**Proof.** A sketch of the proof is given. Let us first consider the case where the blurring scale is  $s = 0$ . Each edge curve  $e_k$  is  $C^2$  and can be covered by a band  $\beta_k$  of width  $\varepsilon^2$ . This band is a union of straight tubes of width  $\varepsilon^2$  and length  $\varepsilon/C$  where  $C$  is the maximum curvature of the edge curves. Each tube is decomposed in two elongated triangles as illustrated in Figure 9.6. The number of such triangles is  $2CL_k\varepsilon^{-1}$  where  $L_k$  is the length of  $e_k$ . Triangle vertices should also be appropriately adjusted at junctions or corners. Let  $L = \sum_k L_k$  be the total length of edges and  $\beta = \cup_k \beta_k$  be the band covering all edges. This band is divided in  $2CL\varepsilon^{-1}$  triangles. Since  $f$  is bounded,  $\|f - \tilde{f}_M\|_{L^2(\beta)}^2 \leq \text{area}(\beta) \|f\|_\infty^2 \leq L\varepsilon^2 \|f\|_\infty^2$ .

The complementary  $\beta^c = [0, 1]^2 - \beta$  is covered at the center by nearly equilateral triangles of surface of the order of  $\varepsilon$ , as shown in Figure 9.6. There are  $O(\varepsilon^{-1})$  such triangles. Performing this packing requires us to use a boundary layer of triangles that connect the large nearly isotropic triangles of width  $\varepsilon^{1/2}$  to the anisotropic triangles of size  $\sim \varepsilon^2 \times \varepsilon$ , along edges. One can verify that such a boundary layer can be constructed with  $O(LC\varepsilon^{-1})$  triangles. Since  $f$  is  $C^2$  on  $\Omega - \beta$ , the approximation error of a linear interpolation  $\tilde{f}$  over this triangulation is  $\|f - \tilde{f}_M\|_{L^\infty(\beta^c)} = O(\|f\|_{C^2(\beta^c)} \varepsilon^2)$ . Thus, the total error satisfies

$$\|f - \tilde{f}_M\|^2 = O(L\|f\|_\infty^2 \varepsilon^2 + \|f\|_{C^2}^2 \varepsilon^2)$$

with a number of triangles  $M = O((CL + 1)\varepsilon^{-1})$ , which verifies (9.70) for  $s = 0$ .

Suppose now that  $s > 0$ . According to Definition 9.1,  $f = \tilde{f} \star h_s$ , so edges are diffused into sharp transitions along a tube of width  $s$ . Since  $h$  is  $C^2$ , within this tube  $f$  is  $C^2$ , but it has large-amplitude derivatives if  $s$  is small. This defines an overall band  $\beta$  of surface  $Ls$  where the derivatives of  $f$  are potentially large. The triangulation of domain  $[0, 1]^2 - \beta$  can be treated similarly to the case  $s = 0$ . Thus, we concentrate on the triangulation of band  $\beta$  and show that one can find a triangulation with  $O(\varepsilon^{-1})$  triangles that yields an error in  $O(\varepsilon^2)$  over the band.

Band  $\beta$  has a surface  $Ls$  and can thus be covered by  $L\varepsilon^{-1}$  triangles of surface  $\varepsilon s$ . Let us compute the aspect ratio of these triangles to minimize the resulting error. A blurred piecewise  $C^2$  image  $f = \tilde{f} \star h_s$  has an anisotropic regularity at a point  $x$  close to an edge curve  $e_k$  where  $\tilde{f}$  is discontinuous. Let  $\tau_1(x)$  be the unit vector that is tangent to  $e_k$  at point  $x$ , and  $\tau_2(x)$  be the perpendicular vector. In the system of coordinates  $(\tau_1, \tau_2)$ , for

any  $u = u_1, \tau_1 + u_2 \tau_2$  in the neighborhood of  $x$ , one can prove that [342, 365]

$$\left| \frac{\partial^{i_1+i_2} f}{\partial u_1^{i_1} \partial u_2^{i_2}}(u) \right| = O(s^{-i_1/2-i_2}). \quad (9.71)$$

Thus, for  $s$  small the derivatives are much larger along  $\tau_2$  than along  $\tau_1$ . The error of local linear approximation can be computed with a Taylor decomposition

$$f(x + \Delta) = f(x) + \langle \nabla_x f, h \rangle + \frac{1}{2} \langle H_x(f) \Delta, \Delta \rangle + O(\|\Delta\|^2),$$

where  $H_x(f) \in \mathbb{R}^{2 \times 2}$  is the symmetric Hessian tensor of second derivatives. Let us decompose  $\Delta = \Delta_1 \tau_1 + \Delta_2 \tau_2$ :

$$|f(x + \Delta) - (f(x) + \langle \nabla_x f, \Delta \rangle)| = O(s^{-1} |\Delta_1|^2 + s^{-2} |\Delta_2|^2 + s^{-3/2} |\Delta_1| |\Delta_2|). \quad (9.72)$$

For a triangle of width and length  $\Delta_1$  and  $\Delta_2$ , we want to minimize the error for a given surface  $s\varepsilon \sim \Delta_1 \Delta_2$ , which is obtained with  $\Delta_2/\Delta_1 = \sqrt{s}$ . It results that  $\Delta_1 \sim s^{1/3} \varepsilon^{1/2}$  and  $\Delta_2 \sim s^{3/4} \varepsilon^{1/2}$ , which yields a linear approximation error (9.72) on this triangle:

$$|f(x + \Delta) - (f(x) + \langle \nabla_x f, \Delta \rangle)| = O(s^{-1/2} \varepsilon).$$

This gives

$$\|f - \tilde{f}_M\|_{L^2(\beta)}^2 \leq \text{area}(\beta) \|f - \tilde{f}_M\|_\infty^2 = O(L\varepsilon^2).$$

It proves that the  $O(\varepsilon^{-1})$  triangles produce an error of  $O(\varepsilon^2)$  on band  $\beta$ . Since the same result is valid on  $[0, 1]^2 - \beta$ , it yields (9.70). ■

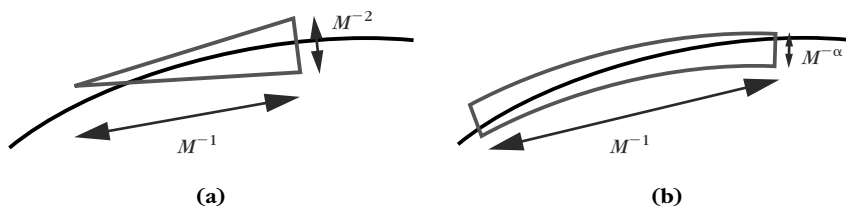
This theorem proves that an adaptive triangulation can yield an optimal decay rate  $O(M^{-2})$  for a piecewise  $C^2$  image. The decay rate of the error is independent from the blurring scale  $s$ , which may be zero or not. However, the triangulation depends on  $s$  and on the edge geometry.

Wherever  $f$  is uniformly  $C^2$ , it is approximated over large, nearly isotropic triangles of size  $O(M^{1/2})$ . In the neighborhood of edges, to introduce an error  $O(M^{-2})$ , triangles must be narrow in the direction of the discontinuity and as long as possible to cover the discontinuity with a minimum number of triangles. Since edges are  $C^2$ , they can be covered with triangles of width and length proportional to  $M^{-2}$  and  $M^{-1}$ , as illustrated in Figure 9.7.

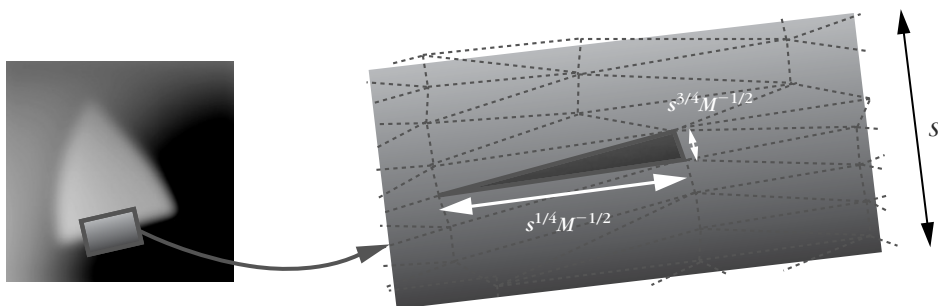
If the image is blurred at a scale  $s$ , then the discontinuities are a diffused neighborhood of size  $s$  where the image has sharp transitions. Theorem 9.19 shows that the tube of width  $s$  around each edge should be covered with triangles of a width and length proportional to  $s^{3/4} M^{-1/2}$  and  $s^{1/4} M^{-1/2}$ , as illustrated in Figure 9.8.

### Algorithms to Design Adapted Triangulations

It is difficult to adapt the triangulation according to Theorem 9.19 because the geometry of edges and the blurring scale  $s$  are unknown. There is currently no adaptive triangulation algorithm that guarantees finding an approximation with an error decay of  $O(M^{-2})$  for all piecewise  $C^2$  images. Most algorithms use greedy strategies

**FIGURE 9.7**

(a) Adapted triangle and (b) finite element to approximate a discontinuous function around a singularity curve.

**FIGURE 9.8**

Aspect ratio of triangles for the approximation of a blurred contour.

that iteratively construct a triangulation by progressively reducing the approximation error. Some algorithms progressively increase the number of triangles, while others decimate a dense triangulation.

Delaunay refinement algorithms, introduced by Ruppert [421] and Chew [160], proceed by iteratively inserting points to improve the triangulation precision. Each point is added at a circumcenter of one triangle, and is chosen to reduce the approximation error as much as possible. These algorithms control the shape of triangles and are used to compute isotropic triangulations of images where the size of the triangles varies to match the local image regularity. Extensions of these vertex insertion methods capture anisotropic regularity by locally modifying the notion of circumcenter [337] or with a local optimization of the vertex location [77].

Triangulation-thinning algorithms start with a dense triangulation of the domain and progressively remove either a vertex, an edge, or a face to increase the approximation error as slowly as possible until  $M$  triangles remain [238, 268, 305]. These methods do not control the shape of the resulting triangles, but can create effective anisotropic approximation meshes. They have been used for image compression [205, 239].

These adaptive triangulations are most often used to mesh the interior of a two- or three-dimensional domain having a complex boundary, or to mesh a two-dimensional surface embedded in three-dimensional space.

### Approximation of Piecewise $C^\alpha$ Images

Adaptive triangulations could be generalized to higher-order approximations of piecewise  $C^\alpha$  images to obtain an error in  $O(M^{-\alpha})$  with  $M$  finite elements for  $\alpha > 2$ . This would require computing polynomial approximations of order  $p = \lceil \alpha \rceil - 1$  on each finite element, and the support of these finite elements should also approximate the geometry of edges at an order  $p$ . To produce an error  $\|f - f_M\|^2 = O(M^{-\alpha})$ , it is indeed necessary to cover edge curves with  $O(M)$  finite elements of width  $O(M^{-\alpha})$ , as illustrated in Figure 9.7. However, this gets extremely complicated and has never been implemented numerically. Section 12.2.4 introduces bandlet approximations, which reach the  $O(M^{-\alpha})$  error decay for piecewise  $C^\alpha$  images, by choosing a best basis in a dictionary of orthonormal bases.

### 9.3.3 Curvelet Approximations

Candès and Donoho [135] showed that a simple thresholding of curvelet coefficients yields nearly optimal approximations of piecewise  $C^2$  images, as opposed to a complex triangulation optimization.

Section 5.5.2 introduced curvelets, defined with a translation, rotation, and anisotropic stretching

$$c_{2j,u}^\theta(x_1, x_2) = c_{2j}(R_\theta(x - u)) \quad \text{where} \quad c_{2j}(x_1, x_2) \approx 2^{-3j/4} c(2^{-j/2}x_1, 2^{-j}x_2), \quad (9.73)$$

where  $R_\theta$  is the planar rotation of angle  $\theta$ . A curvelet  $c_{j,m}^\theta$  is elongated in the direction  $\theta$ , with a *width* proportional to its *length*<sup>2</sup>. This parabolic scaling corresponds to the scaling of triangles used by Theorem 9.19 to approximate a discontinuous image along  $C^2$  edges.

A tight frame  $\mathcal{D} = \{c_{j,m}^\theta\}_{j,m,\theta}$  of curvelets  $c_{j,m}^\theta(x) = c_{2j}^\theta(x - u_m^{(j,\theta)})$  is obtained with  $2^{-\lfloor j/2 \rfloor + 2}$  equispaced angles  $\theta$  at each scale  $2^j$ , and a translation grid defined by

$$\forall m = (m_1, m_2) \in \mathbb{Z}^2, \quad u_m^{(j,\theta)} = R_\theta(2^{j/2}m_1, 2^j m_2). \quad (9.74)$$

This construction yields a tight frame of  $\mathbf{L}^2[0, 1]^2$  with periodic boundary conditions [135].

An  $M$ -term thresholding curvelet approximation is defined by

$$f_M = \sum_{(\theta,j,m) \in \Lambda_T} \langle f, c_{j,m}^\theta \rangle c_{j,m}^\theta \quad \text{with} \quad \Lambda_T = \left\{ (j, \theta, m) : |\langle f, c_{j,m}^\theta \rangle| > T \right\},$$

where  $M = |\Lambda_T|$  is the number of approximation curvelets. Since curvelets define a tight frame with a frame bound of  $A > 0$ ,

$$\|f - f_M\|^2 \leq A^{-1} \sum_{(\theta,j,m) \notin \Lambda_T} |\langle f, c_{j,m}^\theta \rangle|^2. \quad (9.75)$$

Although the frame is tight, this is not an equality because the thresholded curvelet coefficients of  $f$  are not the curvelet coefficients of  $f_M$  due to the frame redundancy. Theorem 9.20 shows that a thresholding curvelets approximation of a piecewise  $\mathbf{C}^2$  image has an error with a nearly optimal asymptotic decay.

**Theorem 9.20:** *Candès, Donoho.* Let  $f$  be a piecewise  $\mathbf{C}^2$  image. An  $M$ -term curvelet approximation satisfies

$$\|f - f_M\|^2 = O(M^{-2}(\log M)^3). \quad (9.76)$$

**Proof.** The detailed proof can be found in [135]. We give the main ideas by analyzing how curvelet atoms interact with regular parts and with edges in a piecewise regular image. The blurring  $f = \bar{f} * h_s$  is nearly equivalent to translating curvelet coefficients from a scale  $2^j$  to a scale  $2^j + s$ , and thus does not introduce any difficulty in the approximation. In the following, we suppose that  $s = 0$ .

The approximation error (9.76) is computed with an upper bound on the energy of curvelet coefficients (9.75). This sum is divided in three sets of curvelet coefficients. Type I curvelets have a support mostly concentrated where the image is uniformly  $\mathbf{C}^2$ ; these coefficients are small. Type II curvelets are in a neighborhood of an edge, and are elongated along the direction of the tangent to the edge; these coefficients are large. Type III curvelets are in a neighborhood of an edge with an angle different from the tangent angle; these coefficients get quickly small as the difference of angle increases. An upper bound of the error is computed by selecting the largest  $M/3$  curvelet coefficients for each type of curvelet coefficient and by computing the energy of the leftover curvelet coefficients for each type of coefficient.

A type I curvelet is located at a position  $u_m^{(j,\theta)}$  at a distance larger than  $K 2^{j/2}$  from edges. Since curvelets have vanishing moments, keeping type I curvelets at scales larger than  $2^j$  is equivalent to implementing a linear wavelet approximation at a scale  $2^j$ . Theorem 9.16 shows that for linear wavelet approximations of  $\mathbf{C}^2$  images, keeping  $M/3$  larger-scale coefficients yields an error that decreases like  $O(M^{-2})$ .

For type II curvelets in the neighborhood of an edge, with an angle  $\theta$  aligned with the local direction of the tangent to the edge, the sampling interval in this direction is also  $2^{j/2}$ . Thus, there are  $O(L 2^{-j/2})$  type II curvelets along the edge curves of length  $L$  in the image. These curvelet coefficients are bounded:

$$|\langle f, c_{j,m}^\theta \rangle| \leq \|f\|_\infty \|c_{2^j}\|_1 = \|f\|_\infty O(2^{3j/4})$$

because  $c_{2^j}(x_1, x_2) \approx 2^{-3j/4} c(2^{-j}x_1, 2^{-j/2}x_2)$ . If we keep the  $M/3$  larger-scale type II curvelets, since there are  $O(L 2^{-j/2})$  such curvelets at each scale, it amounts to keeping them at scales above  $2^l = O(L^2 M^{-2})$ . The leftover type II curvelets have an energy  $O(L 2^{-l/2}) \|f\|_\infty^2 O(2^{3l/2}) = O(M^{-2})$ .

Type III curvelet coefficients  $|\langle f, c_{j,m}^\theta \rangle|$  are located in the neighborhood of an edge with an angle  $\theta$  that deviates from the local orientation  $\theta_0$  of the edge tangent. The coefficients have a fast decay as  $|\theta - \theta_0|$  increases. This is shown in the Fourier domain by verifying that the Fourier domain where the energy of the localized edge patch is concentrated becomes increasingly disjoint from the Fourier support of  $\hat{c}_{j,m}^\theta$  as  $|\theta - \theta_0|$  increases. The error analysis of these curvelet coefficients is the most technical aspect of the proof. One can prove that selecting the  $M/3$  type III largest curvelets yields an error

among type III curvelets that is  $O(M^{-2}(\log_2 M)^3)$  [135]. This error dominates the overall approximation error and yields (9.76). ■

The curvelet approximation rate is optimal up to a  $(\log_2 M)^3$  factor. The beauty of this result comes from its simplicity. Unlike an optimal triangulation that must adapt the geometry of each element, curvelets define a fixed frame with coefficients that are selected by a simple thresholding. However, this simplicity has a downside. Curvelet approximations are optimal for piecewise  $C^\alpha$  images for  $\alpha = 2$ , but they are not optimal if  $\alpha > 2$  or  $\alpha < 1$ . In particular, curvelets are not optimal for bounded variation functions and their nonlinear approximation error does not have the  $M^{-1}$  decay of wavelets. Irregular geometric structures and isolated singularities are approximated with more curvelets than wavelets. Section 12.2.4 studies approximations in bandlet dictionaries, which are adapted to the unknown geometric image regularity.

In most images, curvelet frame approximations are not as effective as wavelet orthonormal bases because they have a redundancy factor  $A$  that is at least 5, and because most images include some structures that are more irregular than just piecewise  $C^2$  elements. Section 11.3.2 describes curvelet applications to noise removal.

## 9.4 EXERCISES

- 9.1** <sup>2</sup> Suppose that  $\{g_m\}_{m \in \mathbb{Z}}$  and  $\{\tilde{g}_m\}_{m \in \mathbb{Z}}$  are two dual frames of  $L^2[0, 1]$ .
- Let  $f_N = \sum_{m=0}^{N-1} \langle f, g_m \rangle \tilde{g}_m$ . Prove that the result (9.4) of Theorem 9.1 remains valid.
  - Let  $\langle f, g_{m_k} \rangle$  be the coefficient of rank  $k$ :  $|\langle f, g_{m_k} \rangle| \geq |\langle f, g_{m_{k+1}} \rangle|$ . Prove that if  $|\langle f, g_{m_k} \rangle| = O(k^{-s})$  with  $s > 1/2$ , then the best approximation  $f_M$  of  $f$  with  $M$  frame vectors satisfies  $\|f - f_M\|^2 = O(M^{1-2s})$ .
- 9.2** <sup>1</sup> *Color images.* A color pixel is represented by red, green, and blue components  $(r, g, b)$ , which are considered as orthogonal coordinates in a three-dimensional color space. The red  $r[n_1, n_2]$ , green  $g[n_1, n_2]$ , and blue  $b[n_1, n_2]$  image pixels are modeled as values taken by, respectively, three random variables  $R$ ,  $G$ , and  $B$ , which are the three coordinates of a color vector. Estimate numerically the  $3 \times 3$  covariance matrix of this color random vector from several images and compute the Karhunen-Loëve basis that diagonalizes it. Compare the color images reconstructed from the two Karhunen-Loëve color channels of highest variance with a reconstruction from the red and green channels.
- 9.3** <sup>2</sup> Suppose that  $\mathcal{B} = \{g_m\}_{m \in \mathbb{Z}}$  and  $\tilde{\mathcal{B}} = \{\tilde{g}_m\}_{m \in \mathbb{Z}}$  are two dual frames of  $L^2[0, 1]$ . Let  $f_N = \sum_{m=0}^{N-1} \langle f, g_m \rangle \tilde{g}_m$ . Prove that the result (9.4) of Theorem 9.1 remains valid even though  $\mathcal{B}$  is not an orthonormal basis.

- 9.4** <sup>2</sup> Let  $\vec{f} = (f_k)_{0 \leq k < K}$  be a multichannel signal where each  $f_k$  is a signal of size  $N$ . We write  $\|\vec{f}\|_F^2 = \sum_{k=0}^{K-1} \|f_k\|^2$ . Let  $\vec{f}_M = (f_{k,M})_{0 \leq k < K}$  be the multichannel signal obtained by projecting all  $f_k$  on the same  $M$  vectors of an orthonormal basis  $\mathcal{B} = \{g_m\}_{0 \leq m < N}$ . Prove that the best  $M$ -term approximation  $\vec{f}_M$  that minimizes  $\|\vec{f} - \vec{f}_M\|_F^2$  is obtained by selecting the  $M$  vectors  $g_m \in \mathcal{B}$  that maximize  $\sum_{k=0}^{K-1} |\langle f_k, g_m \rangle|^2$ .
- 9.5** <sup>1</sup> Verify that for  $f = C \mathbf{1}_{[0,1/2]}$ , a linear approximation with the  $N$  largest scale wavelets over  $[0, 1]$  produces an error that satisfies  $\varepsilon_l(N, f) \sim \|f\|_V^2 N^{-1}$ .
- 9.6** <sup>2</sup> Prove that for any  $f \in \mathbf{L}^2[0, 1]$ , if  $\|f\|_V < +\infty$ , then  $\|f\|_\infty < +\infty$ . Verify that one can find an image  $f \in \mathbf{L}^2[0, 1]^2$  such that  $\|f\|_V < +\infty$  and  $\|f\|_\infty = +\infty$ .
- 9.7** <sup>2</sup> Prove that if  $f \in \mathbf{W}^s(\mathbb{R})$  with  $s > p + 1/2$ , then  $f \in \mathbf{C}^p$ .
- 9.8** <sup>2</sup> The family of discrete polynomials  $\{p_k[n] = n^k\}_{0 \leq k < N}$  is a basis of  $\mathbb{C}^N$ .
  - Implement numerically a Gram-Schmidt algorithm that orthogonalizes  $\{p_k\}_{0 \leq k < N}$ .
  - Let  $f$  be a signal of size  $N$ . Compute the polynomial  $f_k$  of degree  $k$  that minimizes  $\|f - f_k\|$ . Perform numerical experiments on signals  $f$  that are uniformly smooth and piecewise smooth. Compare the approximation error with the error obtained by approximating  $f$  with the  $k$  lower-frequency Fourier coefficients.
- 9.9** <sup>3</sup> Let  $f$  be a function with a finite total variation  $\|f\|_V$  on  $[0, 1]$ . For a quantization step  $\Delta$ ,  $[0, 1]$  is divided into consecutive intervals  $[t_k, t_{k+1}]$  with  $m\Delta \leq f(t) \leq (m+1)\Delta$  for  $t \in [t_k, t_{k+1}]$ . In each  $[t_k, t_{k+1}]$ ,  $f(t)$  is approximated by its average  $a_k = (t_{k+1} - t_k)^{-1} \int_{t_k}^{t_{k+1}} f(t) dt$ . Let  $M$  be the total number of such intervals and  $f_M(t) = a_k$  for  $t \in [t_k, t_{k+1}]$  be a piecewise constant approximation of  $f$ . Prove that there exists a constant  $C$  such that
- $$\|f - f_M\|^2 \leq C \|f\|_V^2 M^{-2}.$$
- 9.10** <sup>3</sup> Let  $\alpha[M]$  be a decreasing sequence such that  $\lim_{M \rightarrow +\infty} \alpha[M] = 0$ . By using (9.61) prove that there exists a bounded variation function  $f \in \mathbf{L}^2[0, 1]^2$  such that  $\varepsilon_l(f, M) \geq \alpha[M]$  (the amplitude of  $f$  is not bounded).
- 9.11** <sup>1</sup> Consider a wavelet basis of  $\mathbf{L}^2[0, 1]$  constructed with wavelets having  $q > s$  vanishing moments and that are  $\mathbf{C}^q$ . Construct functions  $f \in \mathbf{W}^s[0, 1]$  for which the linear and nonlinear approximation errors in this basis are identical:  $\varepsilon_l(f, M) = \varepsilon_n(f, M)$  for any  $M \geq 0$ .
- 9.12** <sup>2</sup> Let  $f(t)$  be a piecewise polynomial signal of degree 3 defined on  $[0, 1]$ , with  $K$  discontinuities. We denote by  $f_{l,M}$  and  $f_{n,M}$ , respectively, the linear and nonlinear approximations of  $f$  from  $M$  vectors chosen from a Daubechies wavelet basis of  $\mathbf{L}^2[0, 1]$ , with four vanishing moments.
  - Give upper bounds as a function of  $K$  and  $M$  of  $\|f - f_{l,M}\|^2$  and  $\|f - f_{n,M}\|^2$ .

- (b) The Piece-polynomial signal  $f$  in WAVELAB is piecewise polynomial with degree 3. Decompose it in a Daubechies wavelet basis with four vanishing moments, and compute  $\|f - f_K\|$  and  $\|f - \tilde{f}_K\|$  as a function of  $K$ . Verify your analytic formula.

**9.13** <sup>2</sup> Let  $f[n]$  be defined over  $[0, N]$ . We denote by  $f_{p,k}[n]$  the signal that is piecewise constant on  $[0, k]$ , takes at most  $p$  different values, and minimizes

$$\varepsilon_{p,k} = \|f - f_{p,k}\|_{[0,k]}^2 = \sum_{n=0}^k |f[n] - f_{p,k}[n]|^2.$$

- (a) Compute as a function of  $f[n]$  the value  $a_{l,k}$  that minimizes  $c_{l,k} = \sum_{n=l}^k |f[n] - a_{l,k}|^2$ .
- (b) Prove that

$$\varepsilon_{p,k} = \min_{l \in [0, k-1]} \{\varepsilon_{p-1,l} + c_{l,k}\}.$$

Derive a bottom-up algorithm that computes progressively  $f_{p,k}$  for  $0 \leq k \leq N$  and  $1 \leq p \leq K$ , and obtains  $f_{K,N}$  with  $O(KN^2)$  operations. Implement this algorithm in WAVELAB.

- (c) Compute the nonlinear approximation of  $f$  with the  $K$  largest-amplitude Haar wavelet coefficients and the resulting approximation error. Compare this error with  $\|f - f_{K,N}\|$  as a function of  $K$  for the lady and the Piece-polynomial signals in WAVELAB. Explain your results.

**9.14** <sup>2</sup> *Approximation of oscillatory functions:*

- (a) Let  $f(t) = a(t) \exp[i\phi(t)]$ . If  $a(t)$  and  $\phi'(t)$  remain nearly constant on the support of  $\psi_{j,n}$ , then show with an approximate calculation that

$$\langle f, \psi_{j,n} \rangle \approx a(2^j n) \sqrt{2^j} \hat{\psi}(2^j \phi'(2^j n)). \quad (9.77)$$

- (b) Let  $f(t) = \sin t^{-1} \mathbf{1}_{[-1/\pi, 1/\pi]}(t)$ . Show that the  $\ell^p$  norm of the wavelet coefficients of  $f$  is finite if and only if  $p < 1$ . Use the approximate formula.
- (c) Compute an upper bound of the nonlinear approximation error  $\varepsilon_n(f, M)$  of  $\sin t^{-1}$  from  $M$  wavelet coefficients. Verify your theoretical estimate with a numerical calculation in WAVELAB.